Tetrahedron: *Asymmetry* 28 (2017) 1717–1732

Contents lists available at ScienceDirect

Tetrahedron: *Asymmetry*

journal homepage: www.elsevier.com/locate/tetasy

Lipase-catalyzed kinetic resolution approach toward enantiomerically enriched 1-(β-hydroxypropyl)indoles

Paweł Borowiecki [a,*], Iwona Justyniak [b], Zbigniew Ochal [a,*]

[a] *Warsaw University of Technology, Faculty of Chemistry, Department of Drugs Technology and Biotechnology, Koszykowa St. 3, 00-664 Warsaw, Poland*
[b] *Institute of Physical Chemistry, Polish Academy of Sciences, Kasprzaka St. 44/52, 01-224 Warsaw, Poland*

ARTICLE INFO

Article history:
Received 17 August 2017
Revised 25 August 2017
Accepted 18 October 2017
Available online 22 November 2017

ABSTRACT

In a route towards enantiomerically enriched 1-(β-hydroxypropyl)indoles, which are potentially useful building blocks for high value-added chemicals synthesis, a kinetic resolution approach by means of lipase-catalyzed enantioselective acylation as well as hydrolysis/methanolysis has been elaborated for the first time. The enzymatic resolution of chiral *N*-substituted indole-based *sec*-alcohols was successfully accomplished, yielding both enantiomeric forms of the employed derivatives with up to >99% enantiomeric purity via an enantioselective transesterification under mild reaction conditions. The most selective resolutions were obtained using fungal (CAL-B and TLL) and bacterial (PFL and BCL) lipases and vinyl acetate as the acyl group donor. The synthetic protocol described herein is very simple, user-friendly and efficient, thus paving the way for future access towards more complex compounds of this type. The absolute configurations of novel enantiomeric derivatives, and thus stereoselectivity of the described enzymatic reactions were confirmed by application of CDA-based NMR methodology and single-crystal X-ray diffraction analysis.

1. Introduction

Indole chemistry has been used for over 100 years since 1883 in the pioneering useful protocol of so-called '*Fischer indole synthesis*'.[1] A tremendous amount of effort has been directed toward adaptation of the classical Fischer methodology, as well as the development of more efficient and versatile synthetic attempts to obtain indoles.[2] Furthermore, since the indole backbones are particularly desirable in modern organic synthesis, many innovative protocols to prepare[3] and transform[4] them into highly functionalized molecules have been published. The indole motif is present in a large family of natural compounds with a wide range of structural diversity and biological activity. In this regard, over the past few decades a plethora of synthetic campaigns, encompassing significant knowledge of how to obtain a variety of structurally complex and challenging alkaloids of plant,[5] marine,[6] fungal,[7] and bacterial[8] origin, as well as natural and semi-synthetic triptans[9] has been widely elaborated. Moreover, since many of the indole-ring-containing derivatives play an important role in physiological and biochemical processes of living organisms, they have attracted considerable attention for their application in the pharmaceutical industry. In this context, the indole scaffold as the privileged structure is present in over 200 of clinically approved drugs.[10] Indole-based molecules are also common building blocks in other countless applications, including catalysis,[11] manufacturing of dyes and pigments,[12] dietary supplements and nutraceuticals,[13] as well as the production of fungicides,[14] veterinary drugs,[15] and fragrance ingredients.[16]

As already mentioned, the indole core has become one of the most utilized structures especially in medicinal chemistry. Therefore, miscellaneous attempts toward novel derivatives with enhanced bioactive properties have been performed and are continuously under evolution each year.[17] In the last two years it has been shown that the indole ring system is a pharmacophore in many pharmacologically relevant compounds across a wide range of therapeutic areas (Fig. 1).

The most common among them are compounds possessing anti-cancer,[18] anti-microbial,[19] anti-viral [including anti-HIV,[20] anti-HCV,[21] anti-Chikungunya virus (anti-CHIKV),[22] anti-varicella zoster virus (anti-VZV),[23] anti-Coxsackie B4 virus[24] etc.], anti-diabetic,[25] anti-parasitic [including anti-leishmanial[26] and anti-trypanosomiasis[27]], and anti-inflammatory[28] activity. The design strategies employed for the synthesis of novel indole-containing

* Corresponding authors. Tel.: +48 22 660 53 42; fax: +48 22 628 27 41 (P.B.); tel.: +48 22 234 73 27; fax: +48 22 628 27 41 (Z.O.).
E-mail addresses: pawel_borowiecki@onet.eu, pborowiecki@ch.pw.edu.pl (P. Borowiecki), zbigniew.ochal.ztibsl@gmail.com, ochal@ch.pw.edu.pl (Z. Ochal).

https://doi.org/10.1016/j.tetasy.2017.10.010
0957-4166/

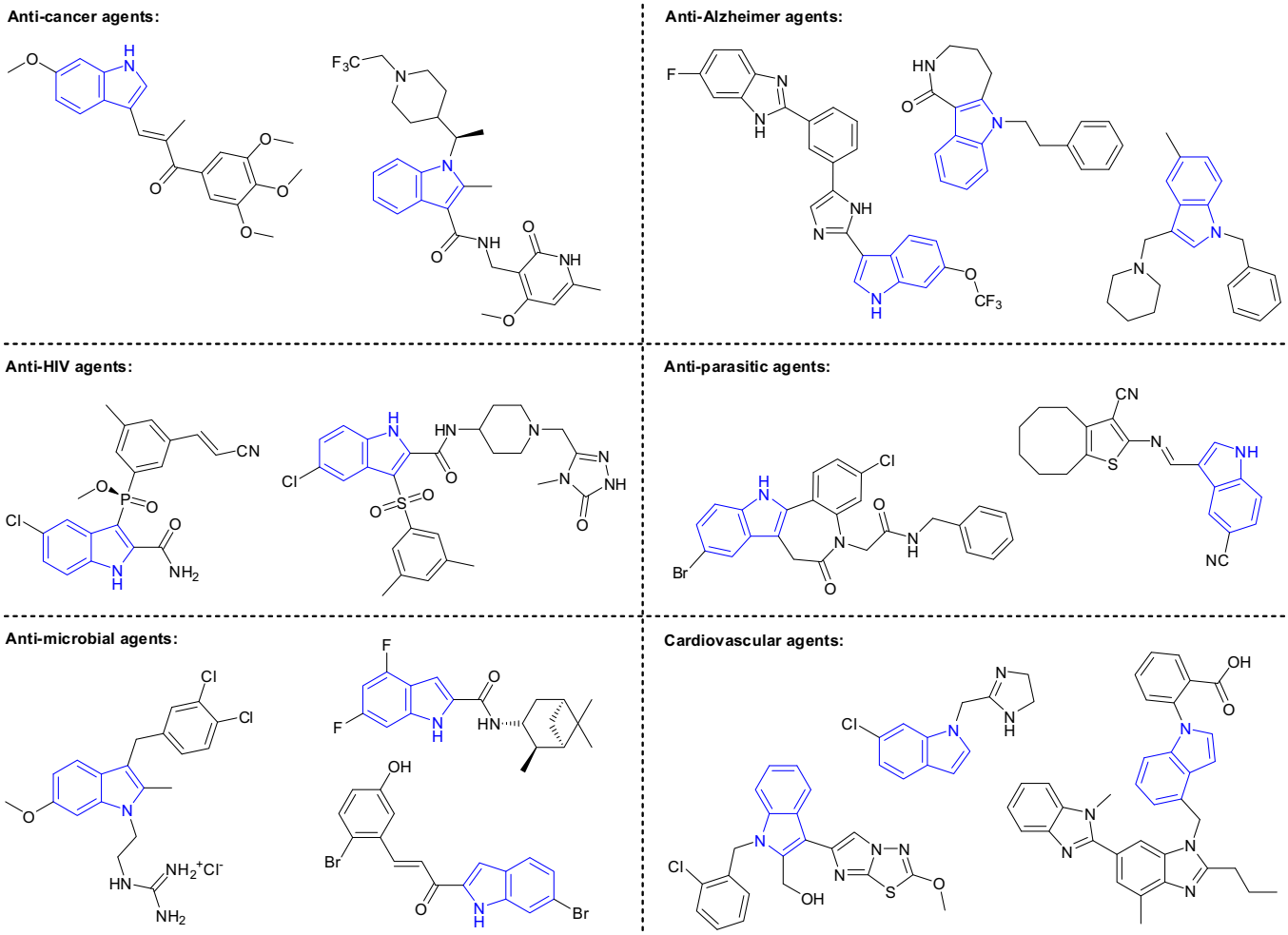

Figure 1. Selected chemical structures of indole-containing compounds currently under clinical investigation.

cardiovascular therapeutics with improved anti-hypertension,[29] anti-platelet,[30] and α-adrenergic[31] activities seem to be very promising options. Besides the above-mentioned bioactive compounds bearing indole moieties, novel derivatives of this kind can be also found in the group of potential therapeutics dedicated to treatment of aging-diseases, such as chronic neurodegenerative Alzheimer's disease,[32] wet age-related macular degeneration[33] or benign prostatic hyperplasia.[34] The results of different studies report that the indole ring is a privileged core structure in many synthetic compounds exhibiting a broad range of other interesting biological activities, such as analgesic,[35] anti-lipidemic,[36] anti-psychotic,[37] and anti-oxidant.[38] Finally, indole scaffold is becoming an important structural component of potential therapeutic agents useful in the treatment of obesity[39] and opioid dependence.[40]

On the other hand, although there are many literature reports on the use of lipases as biocatalysts for the resolution of various heterocyclic secondary alcohols, surprisingly, the role of hydrolytic enzymes regarding chiral indoles of this type is still undeveloped. The described lipase-mediated racemate resolutions have been limited to derivatives structurally closely related to indoles, such as indolines (2,3-dihydroindoles),[41] isoindoles,[42] and carbazoles;[43] however, all of them involve reactions with the amino group instead of the hydroxyl moiety. Herein, we describe the challenge of designing simple enzymatic methodology based on highly stereoselective transformations, mild reaction conditions and low environmental impact for the efficient synthesis of non-racemic *sec*-alcohols with an indole skeleton.

2. Results and discussion

Herein, we continue our efforts toward exploring synergism between chemistry and biochemistry by expanding on novel substrates for biotechnological processes of high scientific importance. Our ultimate goal was to provide a simple and robust approach for utilizing lipase-based biocatalysis for the preparation of three new enantiomerically enriched 1-(β-hydroxypropyl)indoles (*S*)-(+)- and (*R*)-(−)-**3a–c**, which are potentially valuable synthons for manufacturing pharmaceuticals. Scheme 1 outlines the synthetic pathway of chemoenzymatic preparation of non-racemic indole derivatives **3a–c** consisting of classical enzymatic kinetic resolution (Ekinetic resolution, EKR) methodology as a key-step.

2.1. Synthesis of racemic 1-(β-hydroxypropyl)indoles 3a–c

Our initial research focused on preparing the racemic alcohols *rac*-**3a–c** required for enzymatic transformations. In this context, readily available 5-nitro-substituted **1a**, 3-methyl-substituted **1b** and 2,3-dimethyl-substituted indoles **1c** were used as starting materials in the regioselective propylene oxide **2** ring-opening reaction promoted by NaH used in slight excess in dry DMF. After 24 h of stirring at room temperature, the alcohols were finally isolated in moderate (43% for *rac*-**3a**, 56% for *rac*-**3b**) to good (70% for *rac*-**3c**) yields in a straightforward manner. In turn, the racemic indole esters *rac*-**4a–c** and *rac*-**5a–c** requested as the substrates and as analytical standards for enzymatic reaction's progress

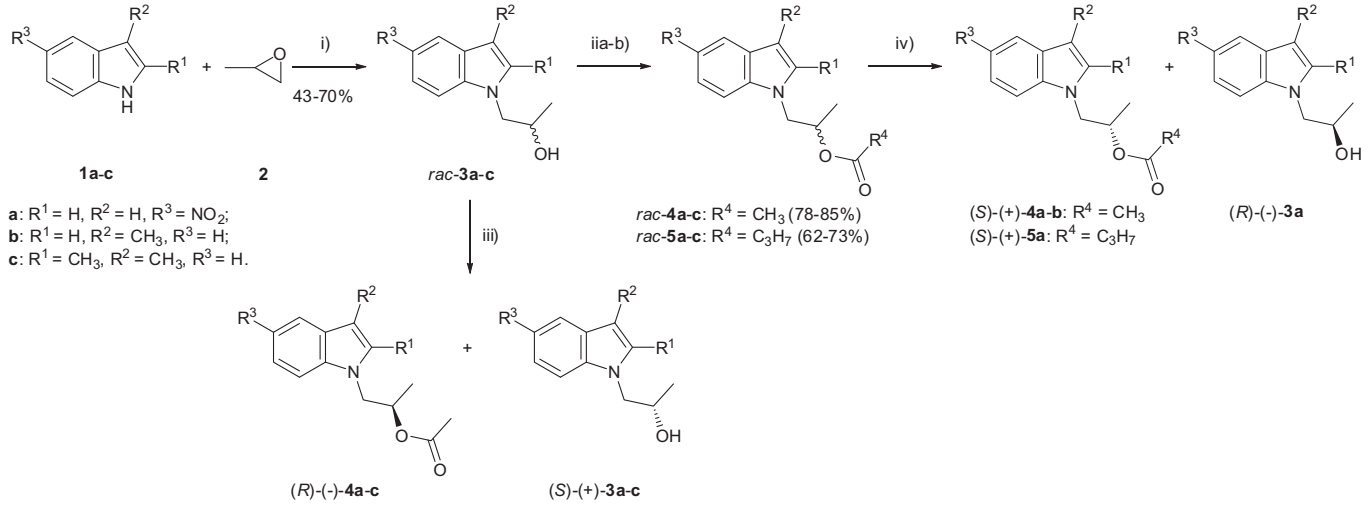

Scheme 1. Lipase-catalyzed kinetic resolution of racemic 1-(β-hydroxypropyl)indoles *rac*-**3a–c** and their esters *rac*-**4a–c** and *rac*-**5a–c**. Reagents and conditions: (i) **2** (1.1 equiv), NaH (1.1 equiv), dry DMF, 20 min at 0–5 °C, then 24 h at RT; (iia) Ac_2O (1.1 equiv), DMAP (cat.), dry CH_2Cl_2, 24 h at RT; (iib) C_3H_7COCl (1.0 equiv), Et_3N (1.0 equiv), DMAP (cat.), dry $PhCH_3$, 24 h at RT; (iii) vinyl acetate (10 equiv) or isopropenyl acetate (10 equiv), lipase (10% w/w), organic solvent, 30 °C, 300 rpm (laboratory shaker); (iv) satd aq TBME or MeOH (10 equiv), lipase (10% w/w), organic solvent, 30 °C, 300 rpm (laboratory shaker).

monitoring and enantiomeric excess (% ee) measurements, were obtained in very good yields (78–85%) for acetates *rac*-**4a–c** and in good yields (62–73%) for butyrates *rac*-**5a–c**, respectively. The esterification reactions were carried out by using 1.1 equiv of acetic anhydride or a stoichiometric amount of butyryl chloride in the presence of 4-dimethylaminopyridine (DMAP) as the acyl transfer catalyst at room temperature for 24 h. In the case of racemic acetates *rac*-**4a–c**, the reactions were performed in dry dichloromethane, and in turn, butyrates *rac*-**5a–c** were prepared in dry toluene solution, into which an equimolar amount of triethylamine as an organic base was added.

2.2. Enzymatic reactions

In order to investigate the activity of the employed enzymes and enantioselectivity (*E*) of the lipase-catalyzed kinetic resolutions, at the outset of enzymatic studies the chromatographic separation conditions for all racemates, including indole alcohols *rac*-**3a–c** and their respective esters *rac*-**4a–c** and *rac*-**5a–c**, were first established (see Supporting Information). The base-line resolution of the enantiomers of all racemic mixtures was successfully accomplished by using only one HPLC chiral column [Chiralcel OD-H (Daicel)]. Moreover, the selected chiral-stationary-phase HPLC conditions led to the separation of both pairs of respective alcohol and ester enantiomers in a single run, which gave us the opportunity to follow the results of kinetic resolution reactions directly from the crude mixtures.

It is well-known that lipase-catalyzed reactions can be implemented in two synthetic variants depending on the reaction medium.[44] They can be carried out in: (i) the aqueous solutions, and/or in (ii) nearly anhydrous organic solvents. The first synthetic option closely mimics the physiological biotransformation pathways of naturally occurring compounds (*i.e.* triglycerides), however such an attempt often leads to unpredictable side-reactions yielding undesired by-products, due to in situ racemization of chiral compounds and limits overall the reaction progress due to low-solubility of the organic substrates. In turn, although the implementation of non-aqueous conditions to a biocatalysis provides an artificial environment for enzymes, such a tactic hopefully offers an extraordinary advantages, amongst which the most important are: (i) the enzymes' ability to catalyze reactions that would be impossible to carry out; (ii) the increase of the enzymes' activity and selectivity in action; and (iii) the incensement of enzymes' thermo-stability and resistance toward proteolytic degradation caused by the simultaneously presence of traces of proteases in technical grade commercial preparations. Moreover, in nearly anhydrous organic solvents: (iv) the scope of potential substrates for enzymes is significantly widened as substrate solubility is improved (this also allows higher substrate loadings); (v) product recovery from organic solvents is relatively simple as compared to water; (vi) the insolubility of enzymes in organic media permits their easy recovery and further reuse; as well as (vii) the catalytic performance is not much influenced by the pH, and finally (viii) space/time yield and volumetric productivity are mostly enhanced. Therefore, to develop a general procedure for the efficient enzymatic kinetic resolution of various indole alcohols *rac*-**3a–c** and their esters *rac*-**4a–c** and *rac*-**5a–c**, and thus to produce both enantiomeric forms of this compounds with high enantiomeric purity, our aim herein was to study the differences in the stereochemical outcome between lipase-catalyzed selective hydrolysis/alcoholysis and lipase-mediated enantioselective O-acylation methodology. Moreover, since in purely aqueous media the non-enzymatic hydrolysis often occur in competition with the enzymatic reaction, therefore, we decided to examine all the hydrolytic attempts (hydrolysis and alcoholysis) in organic solvents using a small amount of water or methanol as the nucleophile, respectively. These biphasic hydrolytic conditions were also applied due to the fact that lipases often show lower catalytic activity in homogeneous aqueous solutions than in the presence of interfaces. Moreover, to avoid the expense and the work, the appropriate optimization of the operating parameters is sufficient to yield a faster and more enantioselective enzymatic reactions. It is however noteworthy that studies on the variation of temperature and mixing speed were ignored by us, and considered to be kept at the same values for each biocatalytic approach, that is 30 °C and 300 rpm, respectively. The reason is two-fold: on the one hand a higher temperature leads to lower enantioselectivity due to the lower difference between energy barriers for two substrate enantiomers occurs, and, on the other hand, although the external mass transfer can be facilitated by increasing the stirring speed, it does not limit the overall reaction rate.

2.2.1. Analytical-scale biotransformations

2.2.1.1. Lipase-catalyzed kinetic resolution of *rac*-3a and its esters. At first, we decided to utilize a lipase-catalyzed hydrolytic methodology. In this regard, 1-(5-nitro-1*H*-indol-1-yl)propan-2-yl acetate *rac*-**4a** and 1-(5-nitro-1*H*-indol-1-yl)propan-2-yl butyrate *rac*-**5a** were employed as the model substrates, and tested under various reaction conditions including enantioselective hydrolysis and alcoholysis (Table 1). In the first set of experiments, several types of common commercial enzyme preparations [5% (w/w) in accordance to substrate], including the typically employed solid-supported lipase B from *Candida antarctica* (CAL-B) available in chemically immobilized form (Novozym 435, Chirazyme L-2, C-2, Lipozyme 435), immobilized lipase from *Thermomyces lanuginosus* (Lipozyme TL-IM, TLL) as well as two the powder native lipases from *Pseudomonas fluorescens* (Amano AK, PFL) and *Burkholderia cepacia* (Amano PS, BCL) were assessed for their catalytic ability. In addition, since *tert*-butyl methyl ether (TBME) has been generally established as one of the most suitable media used in lipase-catalyzed biotransformations of secondary alcohols and their esters, at this step of investigations we decided to carry out all enzymatic reactions only in this solvent. An initial screening of lipases revealed that both native enzymes (Amano AK and Amano PS) were catalytically inactive toward esters *rac*-**4a** and *rac*-**5a**, while all CAL-B preparations exhibited promising activity. To investigate more deeply the stereoselectivity of the (CAL-B)-catalyzed processes, we set the reaction systems at 50 mg scale of the employed substrates *rac*-**4a** and *rac*-**5a**, in TBME saturated with H_2O (for enantioselective hydrolysis) or in TBME with the addition of MeOH as an acyl-group acceptor used in 10-fold molar excess (for enantioselective methanolysis). The reaction progress was traced systematically by taking samples every day and analyzing them chromatographically by GC and chiral HPLC. Screening at slightly elevated temperature (30 °C) revealed that all of the employed CAL-B preparations displayed high *E*-values. In turn, the experiments clearly indicated that the most active lipase from the studied group of biocatalysts is Lipozyme 435, which afforded desired 50% conversion after 3 days. Moreover, the rates of enzymatic methanolysis reactions were significantly higher than those for enantioselective hydrolysis. The differences in enzyme activity concerning those experiments is especially distinguishable for the kinetic resolution of butyric ester *rac*-**5a**. Novozyme 435 and Chirazyme L-2, C-2 both catalyzed the reactions of ester methanolysis faster in ca. 14 days when compared to hydrolytic attempts using water as the nucleophile. In parallel experiments conducted with Lipozyme 435 as the catalyst, the differences between the reaction rates for both biotransformation attempts toward *rac*-**5a** were also significant as the resolution lasted for 14 days less when compared with the kinetic resolution of *rac*-**4a**. It is noteworthy that hydrolytic reactions were much faster for racemic acetate *rac*-**4a** than for butyrate *rac*-**5a** when catalyzed by Novozym 435, and Chirazyme L-2, C-2, but with the exception of Lipozyme 435, which the opposite results were found in the kinetically-controlled esters' methanolysis. In that case, differences in the reaction times required to reach nearly 50% conversions were even more noticeable in favor of kinetic resolutions carried out for butyrate *rac*-**5a** than those proceeded for acetate *rac*-**4a**. In this context, the kinetic resolutions catalyzed by Novozym 435 were 11 days faster (Table 1, entry 2 *vs* entry 4), while the attempts catalyzed by Chirazyme L-2, C-2 lasted approximately 10 days less (Table 1, entry 6 *vs* entry 8). Moreover, when comparing both of the hydrolytic processes for both examined racemic esters, we observed that all three CAL-B lipase preparations displayed higher enantioselectivities when

Table 1
Enantioselective hydrolysis and methanolysis of *rac*-**4a** and *rac*-**5a** under kinetic resolution conditions

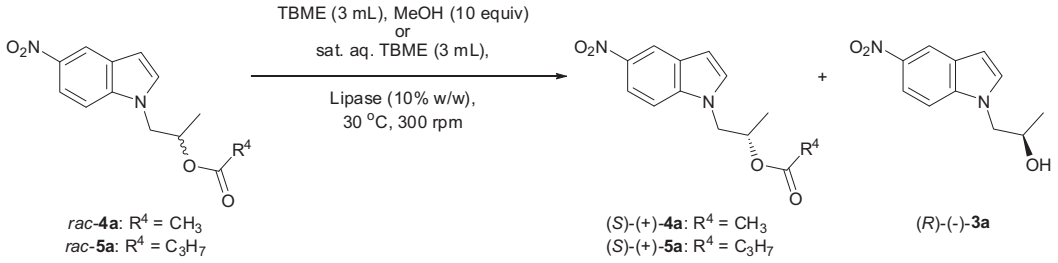

rac-**4a**: $R^4 = CH_3$
rac-**5a**: $R^4 = C_3H_7$
(50 mg)

(*S*)-(+)-**4a**: $R^4 = CH_3$
(*S*)-(+)-**5a**: $R^4 = C_3H_7$

(*R*)-(-)-**3a**

Entry	Lipase	Compound	Nucleophile	*t* [d]	Conv.[e] [%]	ee_s[f] [%]	ee_p[f] [%]	*E*[g]
1	Novozym 435	*rac*-**4a**	H_2O[a]	13	48	82	90	48
2			MeOH[b]	17	53	80	71	14
3		*rac*-**5a**	H_2O[c]	20	51	99	94	170
4			MeOH[d]	6	51	98	96	>200
5	Chirazyme L-2, C-2	*rac*-**4a**	H_2O[a]	15	44	76	98	>200
6			MeOH[b]	16	51	91	88	50
7		*rac*-**5a**	H_2O[c]	20	47	87	99	>200
8			MeOH[d]	6	50	97	96	>200
9	Lipozyme 435	*rac*-**4a**	H_2O[a]	15	46	83	97	172
10			MeOH[b]	9	57	>99	74	34
11		*rac*-**5a**	H_2O[c]	20	42	71	98	>200
12			MeOH[d]	3	51	>99	95	>200

[a] Conditions: *rac*-**4a** 50 mg, lipase 5 mg, satd aq TBME 3 mL, 30 °C, 300 rpm (laboratory shaker).
[b] Conditions: *rac*-**4a** 50 mg, lipase 5 mg, TBME 3 mL, MeOH 77 μL (10 equiv), 30 °C, 300 rpm (laboratory shaker).
[c] Conditions: *rac*-**5a** 50 mg, lipase 5 mg, satd aq TBME 3 mL, 30 °C, 300 rpm (laboratory shaker).
[d] Conditions: *rac*-**5a** 50 mg, lipase 5 mg, TBME 3 mL, MeOH 70 μL (10 equiv), 30 °C, 300 rpm (laboratory shaker).
[e] Based on GC, for confirmation the % conversion was calculated from the enantiomeric excess of the unreacted ester (ee_s) and the product (ee_p) according to the formula conv. = $ee_s/(ee_s + ee_p)$.
[f] Determined by chiral HPLC analysis by using a Chiralcel OD-H column.
[g] Calculated according to Chen et al.,[45] using the equation: $E = \{\ln[(1 - \text{conv.})(1 - ee_s)]\}/\{\ln[(1 - \text{conv.})(1 + ee_s)]\}$.

butyrate *rac*-**5a** was employed as the substrate. Moreover, the best results in terms of enantiomeric excess of optically active acetate (*S*)-(+)-**4a** (>99% ee) and butyrate (*S*)-(+)-**5a** (>99% ee) were obtained in (Lipozyme 435)-mediated methanolysis of the respective racemic esters. In turn, the highest enantioenrichment for (*R*)-(−)-**3a** (99% ee) was achieved when enantioselective hydrolytic kinetic resolution of *rac*-**5a** was catalyzed by Chirazyme L-2, C-2, and stopped at 47% conversion.

Taking into account the above facts concerning the low activity of the studied enzyme preparations under hydrolytic conditions, it is apparent that these reactions are far from being preparative. Therefore, it was worthwhile investigating the reverse process, i.e., the lipase-catalyzed synthesis of the ester; the results are shown in Tables 2 and 3. The evaluation of an alternative protocol based on the kinetic resolution of 1-(5-nitro-1*H*-indol-1-yl)propan-2-ol *rac*-**3a** using a 10-fold molar excess of enol esters as acyl-transfer-reagents was made deliberately since these reagents can significantly accelerate the rate of lipase-mediated reactions. This is mostly due to the fact that such activated esters efficiently shift the equilibrium towards the synthesis of esters by generating side-products, which rapidly tautomerize in situ to give stable carbonyl compounds (acetaldehyde in the case of vinyl esters or acetone in the case of isopropenyl esters). Moreover, the great benefit of this strategy is that the laborious work-up is not required, which stems from the fact that the solid biocatalyst can be removed by simple filtration, and the permeate, after being concentrated, can be directly subjected on column chromatography. This thus reduces operational complexity, time, and the overall cost of the process.

Moreover, due to the well-recognized fact that the nature of the reaction medium is a critical factor for biocatalysis, since it exerts a strong influence on the catalytic performance of the enzymes, an optimization of the lipase activity and enantioselectivity by solvent variation is mandatory for the development of an efficient resolution of stereoisomers. Therefore, we employed three different nonpolar, water-immiscible solvents [toluene ($PhCH_3$), diisopropyl ether (DIPE), and *tert*-butyl methyl ether (TBME)], which usually match to lipase stability requirements, and in which *rac*-**3a** easily forms homogenous solutions. The conversions, enantiomeric excesses of the resulting resolution products as well as the enantioselectivities of the reactions were determined by GC and chiral HPLC analysis, respectively.

The resolution process of *rac*-**3a** was first attempted with the previously used commercial lipase preparations. We found that Amano PS and Amano AK, which both were completely inactive under the hydrolytic conditions applied before, this time furnished the most enantioselective resolutions with the highest possible theoretical values for the *E*-factor (Table 2, entries 8 and 10). The results obtained with those lipases were very promising, since highly selective transformations catalyzed by them yielded both resolution products (*S*)-(+)-**3a** and (*R*)-(−)-**4a** with excellent enantiomeric purity (>99% ee). When comparing the reaction courses for these preparations, the best compromise between conversion and selectivity for the O-acetylation of *rac*-**3a** was achieved with Amano AK suspended in TBME as the co-solvent. In this regard, Amano AK required only 48 h to accomplish the successful resolution of *rac*-**3a**, whereas under the same conditions, the reactions catalyzed by Amano PS proceeded sluggishly, yielding desired homochiral products after only as much as 15 days. On the other hand, although the rest of the investigated lipases catalyzed the kinetic resolutions at similar rates as Amano AK, they displayed lower enantioselectivities, providing the slower reacting enantiomer (*S*)-(+)-**3a** with an excellent enantiomeric excess (99% ee), and its acetylated counterpart (*R*)-(−)-**4a** in enantioenriched form (89% ee). Experimental data for the acetylation of *rac*-**3a** with vinyl acetate in organic solvent revealed that the reaction velocity was the highest when lipases were suspended in DIPE. However, the enantioselectivity was improved when the kinetic resolutions were performed in TBME.

Next, we examined isopropenyl acetate as an acyl group donor in the enantioselective O-acetylation of *rac*-**3a** (Table 3). This was made intentionally since lipases are particularly prone to being hampered by the side-product released in the reactions carried out with vinyl acetate. This is an acetaldehyde which can form a

Table 2
Enantioselective O-acetylation of *rac*-**3a** with vinyl acetate under kinetic resolution conditions

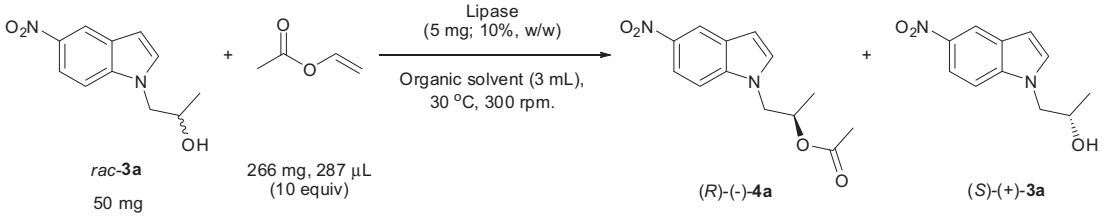

Entry	Lipase[a]	Solvent	*t* [h]	Conv.[b] [%]	ee_s[c] [%]	ee_p[c] [%]	*E*[d]
1	Novozym 435	$PhCH_3$	48	52	89	81	28
2		DIPE	24	47	77	87	33
3		TBME	72	54	99	83	56
4	Chirazyme L-2, C-2	$PhCH_3$	48	53	85	75	19
5		DIPE	24	58	98	71	26
6		TBME	36	53	99	89	90
7	Lipozyme TL-IM	TBME	36	52	91	84	36
8	Amano PS	TBME	360	50	>99	99	≫200
9	Amano AK	$PhCH_3$	48	49	96	>99	≫200
10		TBME	48	50	>99	>99	≫200

[a] Conditions: *rac*-**3a** 50 mg, lipase 5 mg, organic solvent 3 mL, vinyl acetate 287 µL (10 equiv), 30 °C, 300 rpm (laboratory shaker).
[b] Based on GC, for confirmation the% conversion was calculated from the enantiomeric excess of the unreacted alcohol (ee_s) and the product (ee_p) according to the formula conv. = $ee_s/(ee_s + ee_p)$.
[c] Determined by chiral HPLC analysis by using a Chiralcel OD-H column.
[d] Calculated according to Chen et al.,[45] using the equation: $E = \{\ln[(1 - conv.)(1 - ee_s)]\}/\{\ln[(1 - conv.)(1 + ee_s)]\}$.

Table 3
Enantioselective O-acetylation of *rac*-**3a** with isopropenyl acetate in TBME under kinetic resolution conditions

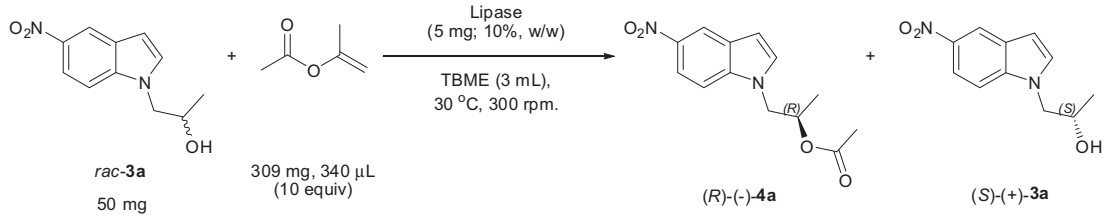

Entry	Lipase[a]	*t* [h]	Conv.[b] [%]	ee$_s$[c] [%]	ee$_p$[c] [%]	*E*[d]
1	Novozym 435	48	52	91	85	39
2	Chirazyme L-2, C-2	32	49	84	87	38
3	Lipozyme TL-IM	48	51	87	83	30
4	Amano PS	192	49	96	99	≫200
5	Amano AK	54	48	93	>99	≫200

[a] Conditions: *rac*-**3a** 50 mg, lipase 5 mg, organic solvent 3 mL, isopropenyl acetate 340 μL (10 equiv), 30 °C, 300 rpm (laboratory shaker).
[b] See footnote of the Table 2.
[c] See footnote of the Table 2.
[d] See footnote of the Table 2.

Schiff base with the amine moiety of the protein amino acid residues (especially lysine residues),[46] and/or simultaneously being oxidized to acetic acid, thus poisoning the catalyst by changing the enzyme ionization state. To avoid such disadvantageous alterations in the micro-environments surrounding the catalytic domain, the less harmful isopropenyl acetate producing inoffensive for the enzyme acetone, seems to be the optimal acyl-transfer-reagent. Of course, it is obvious that disruptions in ionization state affecting enzyme activity can be simply overcome by increasing the catalyst loading, however, we sought to identify optimal conditions for the desired enzymatic systems by using only 10% wt/wt of lipase in respect to substrate *rac*-**3a**, and thus chose innocuous to ester-hydrolyzing enzymes isopropenyl acetate acyl donor reagent.

Taking into consideration the results of earlier performed experiments devoted to solvent selection, we chose TBME as the reaction medium. Again, to afford comparable results, the reactions were stopped as close to 50% substrate conversion as possible according to GC indications, and after subsequent chromatographic isolation, the ee-values were determined by chiral HPLC. Comparing the data from Table 3, it is possible to infer that the lipase-catalyzed kinetic resolution carried out with vinyl acetate was superior to that performed with isopropenyl acetate. From these results, it was also possible to observe that the enzymatic kinetic resolution showed very similar to the aforementioned approach moderate enantioselectivity upon *rac*-**3a** for immobilized CAL-B preparations. In the case of native lipase preparations (Amano AK and Amano PS), the reactions were less selective as the ee-values for the isolated alcohol (*S*)-(+)-**3a** decreased to 93–96% (Table 3, entries 4 and 5). Nevertheless, the enantioenrichment was remarkably high for the formed acetate (*R*)-(−)-**4a**, which was obtained with excellent enantiomeric excess (99–100% ee). The other positive aspect of the kinetic resolution conducted with isopropenyl acetate was that the rate of the acylated product formation in the case of Amano PS was almost two times faster which is somehow intriguing since vinyl esters usually give better reaction rates than isopropenyl esters due to steric reasons. In addition, a similar situation was observed for Novozym 435, which takes 24 h less to convert the substrate when isopropenyl acetate was used as the acyl donor.

2.2.1.2. Lipase-catalyzed kinetic resolution of *rac*-3b and its acetate. The next stage of studies was designed to find the most suitable reaction conditions for the resolution of racemic 1-(3-methyl-1*H*-indol-1-yl)propan-2-yl acetate *rac*-**4b**. For this purpose, the enzymatic kinetic resolution was examined with three different CAL-B preparations previously established as the most potent in water-immiscible (biphasic aqueous−organic) solvent system composed of TBME saturated with water. All of the experimental data regarding hydrolytic approach are summarized in Table 4. As a result, Chirazyme L-2, C-2 was found to hydrolyze *rac*-**4b** with the highest enantioselectivity to furnish optically active alcohol (*R*)-(−)-**3a** with 96% ee, and the remaining acetate (*S*)-(+)-**4b** with 86% ee (Table 4, entry 2). Unfortunately, when analyzing the ee-values and the reaction times it turned out that all lipases have presented worse results upon *rac*-**4b** if compared to the kinetic resolution of *rac*-**4a**. The most active enzyme preparation (Novozym 435) led to low reaction rates affording the desired conversions after as much as 5 days and enantioenriched resolution products with moderate 81–85% ee (Table 4, entry 1). Moreover, for the rest of the studied enzymes, the time required to reach ca. 50% conversion exceeded 23 days (Table 4, entries 2 and 3). In this instance, enantioselective hydrolysis of *rac*-**4b** under kinetically controlled conditions was excluded as being preparative, and thus not studied further.

Again, since the results of lipase-catalyzed hydrolysis of the acetate *rac*-**4b** were not satisfactory, we opted to use the reverse process, i.e., the O-acetylation procedure of the resolution of *rac*-**3b** (Table 5). Initially the reaction system with vinyl acetate (10 equiv) as the source of an acyl group in the presence of 10% wt/wt loading of the appropriate lipase preparation with respect to the substrate *rac*-**3b** at 30 °C was investigated. In general, all experiments of the kinetic resolution of *rac*-**3b** were conducted under the same reaction conditions as described above for the enantioselective O-acetylation of *rac*-**3a**. In this regard, the respective immobilized preparations (Novozym 435, Chirazyme L-2, C-2, Lipozyme 435), and one native lipase (Amano AK) were suspended in three different co-solvents ($PhCH_3$, DIPE, TBME) each. At first glance, a detailed survey on the selection of the optimal lipase catalyst and the solvent upon the acylative kinetic resolution of *rac*-**3b** gave the best results when Amano AK was employed. The most effective resolution mediated by PFL preparation was furnished in DIPE, thus yielding the unreacted alcohol (*S*)-(+)-**3b** with 87% ee and the formed acetate (*R*)-(−)-**4b** with 98% ee (Table 5, entry 11). For (Amano AK)-catalyzed reactions carried out in TBME, the resolution of *rac*-**3b** was obtained with similar conversions as those achieved under the screening conditions of *rac*-**3a**, but with a significantly lower rates, and enantiomeric excesses of both

Table 4
Enantioselective hydrolysis of *rac*-**4b** under kinetic resolution conditions

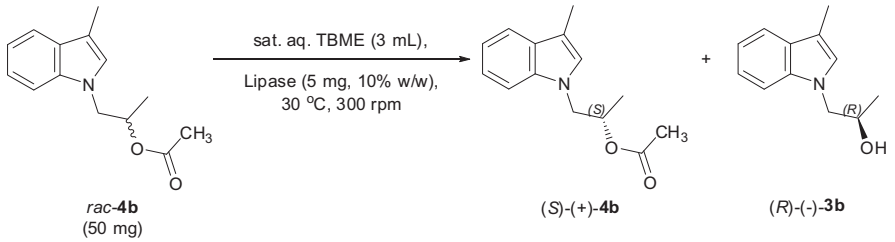

rac-**4b** (50 mg) | (*S*)-(+)-**4b** | (*R*)-(-)-**3b**

Entry	Lipase[a]	*t* [d]	Conv.[b] [%]	ee$_s$[c] [%]	ee$_p$[c] [%]	*E*[d]
1	Novozym 435	5	51	85	81	26
2	Chirazyme L-2, C-2	23	47	86	96	137
3	Lipozyme 435	23	49	89	93	83

[a] Conditions: *rac*-**4b** 50 mg, lipase 5 mg, satd aq TBME 3 mL, 30 °C, 300 rpm (laboratory shaker).
[b] See footnote of the Table 2, but ee$_s$ corresponds to acetate and ee$_p$ to alcohol.
[c] See footnote of the Table 2, but ee$_s$ corresponds to acetate and ee$_p$ to alcohol.
[d] See footnote of the Table 2, but ee$_s$ corresponds to acetate and ee$_p$ to alcohol.

Table 5
Enantioselective O-acetylation of *rac*-**3b** with vinyl acetate under kinetic resolution conditions

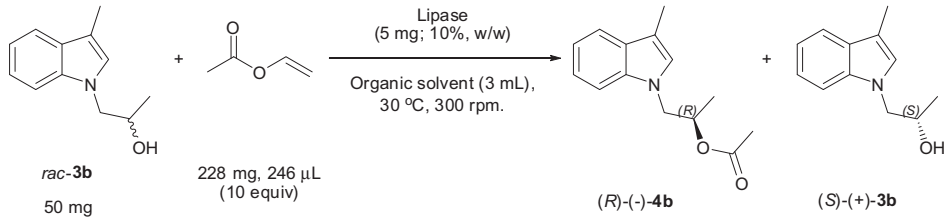

rac-**3b** 50 mg | 228 mg, 246 µL (10 equiv) | (*R*)-(-)-**4b** | (*S*)-(+)-**3b**

Entry	Lipase[a]	Solvent	*t*	Conv.[b] [%]	ee$_s$[c] [%]	ee$_p$[c] [%]	*E*[d]
1	Novozym 435	$PhCH_3$	6 h	42	68	93	56
2		DIPE	4 h	41	59	86	24
3		TBME	5 h	41	66	95	78
4	Chirazyme L-2, C-2	$PhCH_3$	3 h	37	56	94	57
5		DIPE	2 h	41	65	94	63
6		TBME	3 h	41	67	96	99
7	Lipozyme 435	$PhCH_3$	4 h	43	70	93	58
8		DIPE	4 h	36	50	89	28
9		TBME	2 h	42	69	94	67
10	Amano AK	$PhCH_3$	9 d	40	65	98	195
11		DIPE	4 d	47	87	98	>200
12		TBME	4 d	48	88	95	114

[a] Conditions: *rac*-**3b** 50 mg, lipase 5 mg, organic solvent 3 mL, vinyl acetate 246 µL (10 equiv), 30 °C, 300 rpm (laboratory shaker).
[b] See footnote of the Table 2.
[c] See footnote of the Table 2.
[d] See footnote of the Table 2.

kinetic resolution products being obtained in range of 88–95%. In turn, all immobilized CAL-B preparations catalyzed the reactions very efficiently with conversions over 36% achieved after relatively short reaction times (2–6 h) (Table 5, entries 1–9). Under these conditions, optically active acetate (*R*)-(−)-**4b** was obtained with high enantiomeric purity (86–96% ee). In turn, since the reactions catalyzed by CAL-B did not exceed 50% conversion, the enantiomeric excesses for the remaining alcohol (*S*)-(+)-**3b** were moderate (50–87% ee). Lipozyme 435 also appeared to be a quite efficient catalyst reaching 36–43% conversion in a short reaction time (2–4 h), thus affording (*S*)-(+)-**3b** with moderate enantiomeric excess (50–70%) and the acetate (*R*)-(−)-**4b** with high 89–94% ee, respectively. In general, when taking into account the effect of the solvent on the stereochemical outcome, it was clear that the most efficient kinetic resolutions were available in TBME. However, as stated above, the kinetic resolution of *rac*-**3b** in the presence of Amano AK lipase was more efficient when using DIPE. On the other hand, when the reaction was carried out in a less polar solvent ($PhCH_3$, log*P* 2.52), it was slower.

It should be noted that the collected data from the performed experiments gave us detailed insight into the role of the selected lipases under specified conditions, and showed us how the activity of particular enzyme can be controlled to provide the most selective transformations after relatively short reaction times. Nevertheless, the results presented in Table 5 are not sufficient for successful preparative kinetic resolution, and further optimization of the acetylation of *rac*-**3b** was attempted using isopropenyl acetate instead of vinyl acetate. Experimental data for the acylation of *rac*-**3b** with isopropenyl acetate in three different co-solvent systems is shown in Table 6. Based on the results achieved with

Table 6
Enantioselective *O*-acetylation of *rac*-**3b** with isopropenyl acetate under kinetic resolution conditions

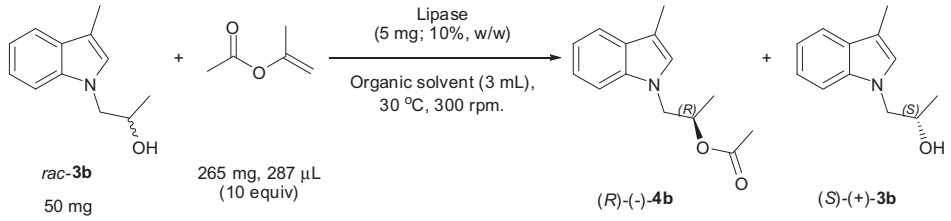

Entry	Lipase[a]	Solvent	t	Conv.[b] [%]	ee_s[c] [%]	ee_p[c] [%]	*E*[d]
1	Novozym 435	$PhCH_3$	7 h	39	59	93	50
2		DIPE	5 h	44	76	96	113
3		TBME	4 h	38	59	95	71
4	Chirazyme L-2, C-2	$PhCH_3$	6 h	35	51	95	65
5		DIPE	5 h	46	80	95	96
6		TBME	3 h	42	70	96	103
7	Lipozyme 435	$PhCH_3$	5 h	41	66	94	64
8		DIPE	3 h	46	80	95	96
9		TBME	3 h	41	66	96	98
10	Amano AK	$PhCH_3$	21 d	<15	N.D.[e]	N.D.[e]	N.D.[e]
11		DIPE	12 d	36	56	98	174
12		TBME	3 d	40	65	98	195

[a] Conditions: *rac*-**3b** 50 mg, lipase 5 mg, organic solvent 3 mL, isopropenyl acetate 287 μL (10 equiv), 30 °C, 300 rpm (laboratory shaker).
[b] Based on GC, for confirmation the% conversion was calculated from the enantiomeric excess of the unreacted alcohol (ee_s) and the product (ee_p) according to the formula conv. = $ee_s/(ee_s + ee_p)$.
[c] Determined by chiral HPLC analysis by using a Chiralcel OD-H column.
[d] Calculated according to Chen et al.,[45] using the equation: $E = \{\ln[(1 - \text{conv.})(1 - ee_s)]\}/\{\ln[(1 - \text{conv.})(1 + ee_s)]\}$.
[e] Not determined.

isopropenyl acetate it was obvious that the most effective resolution occurred in the presence of Amano AK. Both the ether solvents promoted lipase-mediated acetylative kinetic resolution of *rac*-**3b** with comparatively high *E*-values, albeit slightly better conditions in terms of enantiomeric excess of the resolved enantiomers were obtained in TBME. In this solvent, Amano AK catalyzed the kinetic resolution process faster by four orders-of-magnitude when compared with DIPE, furnishing optically active alcohol (*S*)-(+)-**3b** (65% ee) and ester (*R*)-(−)-**4b** (98% ee) with 40% conversion. In general, the enantioselective O-acetylation of *rac*-**3b** with isopropenyl acetate under kinetic resolution conditions mostly lead to a negligible decrease in the catalytic activity and selectivity of the studied enzymes. Similarly as in the kinetic resolution of *rac*-**3b** with vinyl acetate, all CAL-B preparations acted with a high reaction rate, but moderate enantioselectivity. Notwithstanding, two exceptions are worth mentioning. The kinetic resolution of *rac*-**3b** in the presence of Novozym 435 in DIPE was more efficient when using isopropenyl acetate, thus obtaining (*S*)-(+)-**3b** with 76% ee and the formed acetate (*R*)-(−)-**4b** with 96% ee (Table 6, entry 2).

In addition, a slightly improved enantioselectivity toward *rac*-**3b** was also observed when the reaction was carried out in the presence of Chirazyme L-2, C-2 in TBME, attaining 42% conversion after 3 h, and yielding (*S*)-(+)-**3b** with 70% ee and (*R*)-(−)-**4b** with 96% ee (Table 6, entry 6). When comparing both approaches with vinyl acetate and isopropenyl acetate as acyl donors, it was clear that the best enzymatic system for the selective and fast resolution of *rac*-**3b** enantiomers consisted of Amano AK suspended in a mixture of vinyl acetate/DIPE.

2.2.1.3. Lipase-catalyzed kinetic resolution of *rac*-3c. Our next aim was to set up a simple and practical method for the preparation of enantiomerically pure 2,3-dimethyl-substituted indole derivatives (*S*)-(+)-**3c** and (*R*)-(−)-**4c**. For that reason, we decided to extend the described acylative kinetic resolution procedure toward racemic 1-(2,3-dimethyl-1*H*-indol-1-yl)propan-2-ol *rac*-**3c**. At first, the lipase-catalyzed transesterification of *rac*-**3c** was carried out in the presence of commercial CAL-B (Novozym 435, Chirazyme L-2, C-2, Lipozyme 435), TLL (Lipozyme TL-IM) and PFL (Amano AK, the results were omitted for clarity) lipase preparations by using a 10-fold molar excess of vinyl acetate as an acylating agent at 30 °C (Table 7). The experiments gave us valuable information regarding the activity and stereoselectivity of the employed enzymes. It was noticed that in the studied biocatalytic reaction systems, the above-mentioned parameters vary significantly depending on the source of the biocatalyst and the type of solvent. However, among the tested enzymes, the reaction with Novozym 435 undoubtedly displayed the highest enantiomeric ratio (Table 7, entries 1–3). Moreover, the experimental results obtained with Novozym 435 showed that the best chirality inducement occurred when this enzyme was suspended in TBME and the kinetic resolution was continued until the desired 50% conversion was achieved. Under these conditions, the slower-reacting enantiomer (*S*)-(+)-**3c** was isolated in enantiomerically pure form (>99% ee), whereas the acetate (*R*)-(−)-**4c** was afforded with very high 98% ee (Table 7, entry 3). It is worth noting that *rac*-**3c** was less reactive than the previously studied 5-nitro-substituted *rac*-**3a** and 3-methyl-substituted (*rac*-**3b**) derivatives since the transformations lasted 6–24 days. The most active lipases turned out to be Lipozyme 435, which after 6–7 days gave 49% conversion of *rac*-**3c**, thus furnishing the unreacted optically active alcohol (*S*)-(+)-**3c** with 88% ee when suspended in DIPE and 92% ee in TBME, whereas the acetate (*R*)-(−)-**4c** was isolated with 91% ee when the reaction was conducted in DIPE, and with 95% ee if carried out in TBME (Table 7, entries 8–9). Although Amano AK lipase usually gave high activity and enantioselectivity toward previously studied racemic alcohols *rac*-**3a-b**, in a transesterification manner, this time, it was preparatively useless. The collected data also indicate that an additional electron-donating methyl group in the pyr-

Table 7
Enantioselective O-acetylation of *rac*-**3c** with vinyl acetate under kinetic resolution conditions

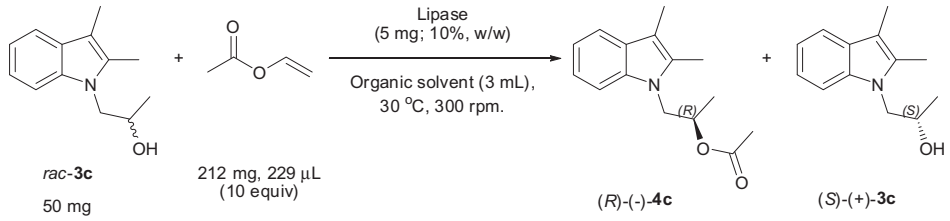

Entry	Lipase[a]	Solvent	*t* [d]	Conv.[b] [%]	ee_s[c] [%]	ee_p[c] [%]	*E*[d]
1	Novozym 435	$PhCH_3$	17	44	76	96	113
2		DIPE	11	48	86	95	109
3		TBME	10	50	>99	98	≫200
4	Chirazyme L-2, C-2	$PhCH_3$	18	51	59	57	6
5		DIPE	13	50	89	90	57
6		TBME	21	47	80	92	59
7	Lipozyme 435	$PhCH_3$	13	40	62	94	61
8		DIPE	7	49	88	91	62
9		TBME	6	49	92	95	129
10	Lipozyme TL-IM	$PhCH_3$	24	8	N.D.[e]	N.D.[e]	N.D.[e]
11		DIPE	9	51	94	91	75
12		TBME	9	51	98	94	149

[a] Conditions: *rac*-**3c** 50 mg, lipase 5 mg, organic solvent 3 mL, vinyl acetate 229 µL (10 equiv), 30 °C, 300 rpm (laboratory shaker).
[b] Based on GC, for confirmation the% conversion was calculated from the enantiomeric excess of the unreacted alcohol (ee_s) and the product (ee_p) according to the formula conv. = $ee_s/(ee_s + ee_p)$.
[c] Determined by chiral HPLC analysis by using a Chiralcel OD-H column.
[d] Calculated according to Chen et al.,[45] using the equation: $E = \{\ln[(1 - \text{conv.})(1 - ee_s)]\}/\{\ln[(1 - \text{conv.})(1 + ee_s)]\}$.
[e] Not determined.

role ring efficiently enhances the substrate activation in reactions catalyzed by Lipozyme TL-IM. It should be note that in the above-mentioned transesterification approaches this enzyme was ineffective, while in the kinetic resolution of *rac*-**3c** preformed in TBME it gave an excellent 98% ee for the recovered optically active alcohol (*S*)-(+)-**3c** and very high 94% ee for the formed acetate (*R*)-(−)-**4c** (Table 7, entry 12). The lowest enantioselectivity was observed for the kinetic resolution reactions catalyzed by Chirazyme L-2, C-2, which yielded the unreacted enantioenriched alcohol (*S*)-(+)-**3c** with ee-values in range of 59–89%, while optically active acetate (*R*)-(−)-**4c** was isolated with 57–92% ee (Table 7, entries 4–6).

In turn, the data of lipase-catalyzed enantioselective transesterification of *rac*-**3c** using isopropenyl acetate as the source of an acetate group are collected in Table 8. The experiments clearly indicated that the best enantiomeric recognition was observed with Novozym 435 suspended in TBME, leading to excellent results in terms of the enantiomeric excess of both kinetic resolution products, yielding (*S*)-(+)-**3c** and (*R*)-(−)-**4c** in almost homochiral forms (up to >99% ee) (Table 8, entry 3). Unexpectedly, substantially better results in comparison to those obtained with vinyl acetate were noticed in the reactions carried out with Chirazyme L-2, C-2 in TBME (Table 8, entry 6). Although still not satisfactory, the rate of this reaction was significantly enhanced affording enantiomerically enriched alcohol (*S*)-(+)-**3c** with 83% ee, and ester (*R*)-(−)-**4c** with 96% ee (Table 8, entry 6). However, in general there are some disadvantages in the use of isopropenyl acetate as in most cases it slowed down the reactions. We found that the tested enzymes exhibited a notably lower activity towards the acetylation of the target racemic substrate *rac*-**3c** especially when suspended in DIPE. For example, the reaction rates of acetate (*R*)-(−)-**4c** formation conducted with Novozym 435, Chirazyme L-2, C-2 and Lipozyme 435 were approximately 9, 8, and 13 days longer than in the case of homologous catalytic systems performed with vinyl acetate as the acyl donor.

2.3. Assignment of the lipases' enantiopreference

In order to verify the stereochemistry of the performed enzymatic reactions, the absolute configuration of the respective resolution products is pivotal. This task is challenging and time-consuming especially if novel compounds with chiral properties are synthesized, and also if they exist in an oil or amorphous state, from which the crystallization of proper crystals is not feasible, and thus X-ray diffraction analysis cannot be performed. To overcome this drawback, various alternative analytical approaches were applied, including NMR spectroscopic investigations carried out mostly by means of chiral derivatization agents (CDAs),[47] chiral solvating agents (CSAs),[48] and lanthanide shift reagents (LSRs),[49] respectively. Moreover, metal complexes and liquid crystals are also employed in NMR spectral investigations, although their application in assignment of absolute stereochemistry is less common.[50] Another well-established technique for absolute configuration determination of optically active compounds is vibrational circular dichroism (VCD),[51] exciton-coupled circular dichroism (ECCD),[52] and vibrational optical activity (VOA).[53] In addition, very practical approach toward absolute configuration assignment of enantioenriched stereogenic centers seems to be so-called Competing Enantioselective Conversion (CEC) method utilizing thin-layer chromatography (TLC).[54]

Of course, it is also reasonable to follow tactics concerning correlation by asymmetric synthesis. For example, These syntheses would require the use of commercially available enantiomerically pure propylene oxide of a defined stereochemistry to obtain analytical standards for the comparison of specific rotation signs and/or pick elution order of chiral gas chromatography (*C*-GC) or chiral high-performance liquid chromatography (*C*-HPLC) analysis, respectively.

Herein, we applied a modified Mosher's methodology described by Riguera et al.[47a] based on NMR spectra of mandelic acid esters of investigated alcohols. The advanced Mosher method is very simple,

Table 8
Enantioselective O-acetylation of *rac*-**3c** with isopropenyl acetate under kinetic resolution conditions

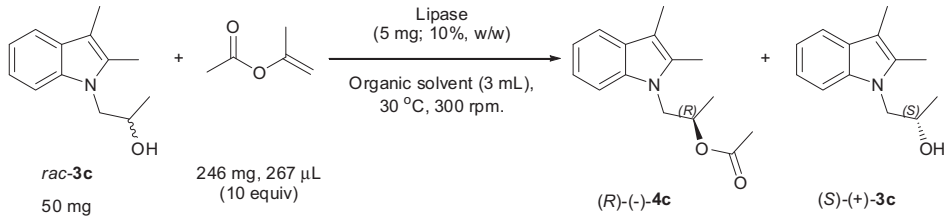

Entry	Lipase[a]	Solvent	*t* [d]	Conv.[b] [%]	ee_s[c] [%]	ee_p[c] [%]	*E*[d]
1	Novozym 435	$PhCH_3$	16	51	92	89	56
2		DIPE	20	49	91	94	103
3		TBME	13	50	>99	99	≫200
4	Chirazyme L-2, C-2	$PhCH_3$	16	40	62	92	45
5		DIPE	21	42	67	91	43
6		TBME	16	46	83	96	128
7	Lipozyme 435	$PhCH_3$	17	45	76	92	55
8		DIPE	20	49	78	81	22
9		TBME	6	48	86	94	90
10	Lipozyme TL-IM	TBME	10	44	76	96	113

[a] Conditions: *rac*-**3c** 50 mg, lipase 5 mg, organic solvent 3 mL, isopropenyl acetate 267 µL (10 equiv), 30 °C, 300 rpm (laboratory shaker).
[b] Based on GC, for confirmation the% conversion was calculated from the enantiomeric excess of the unreacted alcohol (ee_s) and the product (ee_p) according to the formula conv. = $ee_s/(ee_s + ee_p)$.
[c] Determined by chiral HPLC analysis by using a Chiralcel OD-H column.
[d] Calculated according to Chen et al.,[45] using the equation: $E = \{\ln[(1 - conv.)(1 - ee_s)]\}/\{\ln[(1 - conv.)(1 + ee_s)]\}$.

practical, rapid, precise, accurate and reliable for the stereochemistry determination of chiral secondary alcohols.[55] In addition, we have already proven the applicability of this methodology towards wide range of chiral sec-alcohols with heteroaromatic substituent, including imidazole,[56] 1,2,4-triazole,[57] 1,3-benzothiazole,[58] and phenothiazine ring.[59]

In order to determine the absolute configuration of unknown compounds with an indole moiety bearing the secondary carbinol stereogenic centre, one of the investigated alcohol enantiomer (+)-**3c** was independently transformed into two diastereomeric esters **6** and **7** with use of an appropriate chiral auxiliary reagent (Scheme 2). Herein, a double derivatization procedure of (+)-**3c** was performed in dry dichloromethane solution with a stoichiometric amount of (*R*)-(−)- and (*S*)-(+)-α-methoxyphenylacetic acid (MPA) as the CDA reagent using Steglich esterification reaction with dicyclohexylcarbodiimide (DCC) as a coupling reagent and 4-dimethylaminopyridine as a catalyst. After 3 h of stirring at room temperature the two diastereoisomers **6** and **7** were obtained in 85% and 82% yields, respectively.

Next, high-resolution 500 MHz ^{1}H NMR spectra of the resulting MPA-esters **6** and **7** in deuterated chloroform ($CDCl_3$) were recorded and compared. The differences in chemical shifts ($\Delta\delta^{RS}$) of the corresponding protons attached to carbon atoms directly bonded to the stereogenic centre were measured (Fig. 2). The $\Delta\delta^{RS}$ values are crucial for the absolute configuration determination since the sign of the calculated delta parameter (+ or −) carries

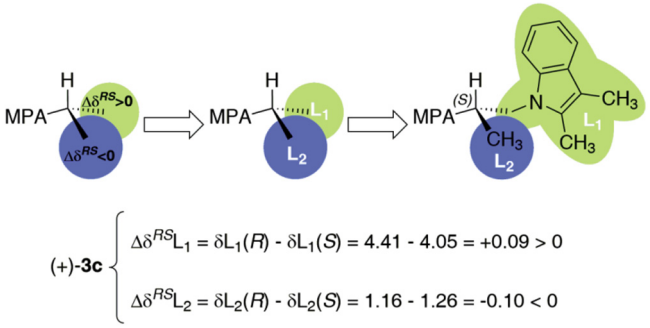

Figure 2. Description of the substituents for assignment of the absolute configuration of (+)-**3c** and $\Delta\delta^{RS}$ values obtained for the MPA-esters **6** and **7**.

the information on the relative position of L_1/L_2 substituents with respect to the anisotropic effect generated by the phenyl group of the MPA unit, which is responsible for an upfield chemical shift (lower frequency) in the NMR spectrum for the spatially proximal protons. The positive $\Delta\delta^{RS}$ value, which corresponds to the signal of the L_1 protons ($\Delta\delta^{RS}L_1 > 0$), and the negative value for the protons belonging to L_2 substituent ($\Delta\delta^{RS}L_2 < 0$) indicate an (*S*)-configuration for the investigated alcohol (+)-**3c** (Fig. 2).

It is worth mentioning that the utility of MPA Mosher's reagent in *sec*-alcohols stereochemistry determination mainly stems from

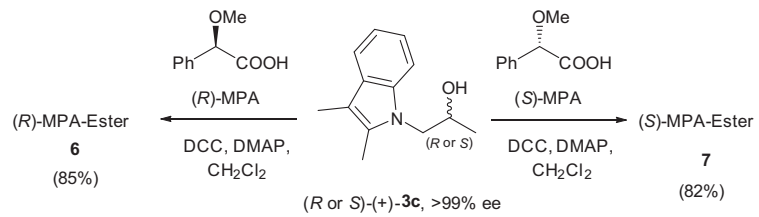

Scheme 2. Transformation of enantiopure alcohol (+)-**3c** using Mosher's reagents [(*R*)- and (*S*)-MPA)] as CDA. Reagents and conditions: (*R*)-(−)-MPA or (*S*)-(+)-MPA (1.0 equiv), DCC (1.0 equiv), DMAP (cat.), dry CH_2Cl_2, 3 h at RT.

the great preference toward the adoption of *syn-periplanar* (*sp*) conformation in the respective rotamer of the formed ester derivative (this phenomenon was empirically confirmed by Latypov et al.[60] using dynamic NMR studies). In this context, the carbinol proton of the methine group of the substrate (+)-**3** part of the ester derivative **6** and **7** as well as the respective Cα carbon, and both the carbonyl and the methoxy group of the MPA unit are all situated in the same plane, whereas the benzene ring is coplanar with the $C_\alpha H$ bond and perpendicular to the C=O bond. This indicates that in the dominant conformer of the MPA-esters both the methoxy and the carbonyl group are in an *sp* disposition (see Newman projections of the appropriate (1*R*,2*S*)- and (1*S*,2*S*)-conformations in diastereomeric esters **6** and **7** depicted in Fig. 3). As can be seen in the Figure 3, the phenyl ring causes shielding of the methyl group protons H(1′) of L2 substituent in (*R*)-MPA-ester **6** and the methylene group protons H(2′) residing within group L1 in the ester with (*S*)-MPA **7**. This result indicates that the absolute configuration of (+)-**3c** at the secondary carbinol stereogenic centre is (*S*)-(+)-**3c**. Analyzing the ^{1}H NMR spectra of the MPA-esters we also observed a unique phenomenon, whereby the inverted influence of anisotropic effect derived from heteroaromatic substituent of the alcoholic (+)-**3** part was responsible for up-fielding the δ-values of both singlets of protons belonging to methoxy and methine group of the MPA moiety. Due to the shielding by the indole ring significant chemical shift differences between those two diastereomers can be found (i.e. $\Delta\delta^{RS}$ = 0.20 ppm for OCH_3 and $\Delta\delta^{RS}$ = 0.21 ppm for protons $C_\alpha H$ adjacent to the corresponding methine centers).

The absolute configurations of the remaining compounds **3a**–**b** were determined by comparison of the specific rotation values exclusively predicated on the assumption that they belong to the homologous series. As it was firmly established by Tschúgaeff,[61] the determination of the absolute configuration on the basis of the specific rotation signs is sufficiently reliable within the scope of similar compounds possessing a single stereogenic center, however, the history of chemistry showed that the validity of such theoretical chemical relationship (correlation) must always be applied with caution.

Therefore, we decided to carry out a thorough study to unequivocally determine the absolute configuration of the (−)-**4a** pure enantiomer obtained from the (Lipozyme 435)-catalyzed enantioselective methanolysis of *rac*-**5a** (Table 1, entry 12). This was performed arbitrarily since only (−)-**4a** gave single crystals of sufficient quality for a XRD structure analysis. With single crystals in hand, we solved the X-ray diffraction structure of (−)-**4a** to be (*R*)-(−)-**4a** (Fig. 4). For details concerning the procedure of (*R*)-(−)-**4a**, single crystal growth conditions and XRD measurements see the Section 4.

After all of the above-mentioned stereochemistry investigations toward indoles with an asymmetric atom of the secondary carbinol

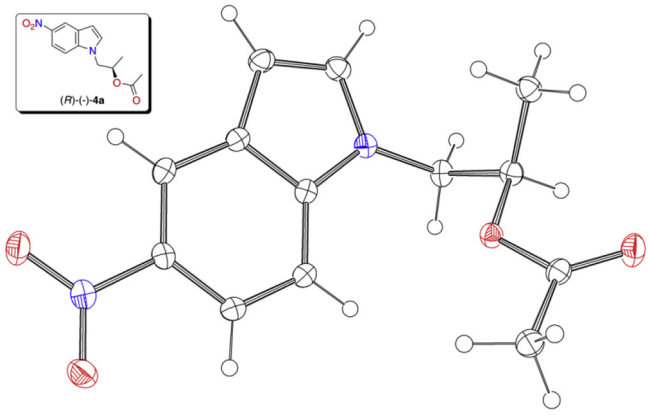

Figure 4. An ORTEP plot of optically pure (*R*)-(−)-1-(5-nitro-1*H*-indol-1-yl)propan-2-yl acetate (*R*)-(−)-**4a**. Thermal ellipsoids were drawn at 50% probability and hydrogen atoms omitted for clarity (C black, H gray, N blue, O red). The following crystal structure has been deposited at the Cambridge Crystallographic Data Centre and allocated the deposition number CCDC-1500811.

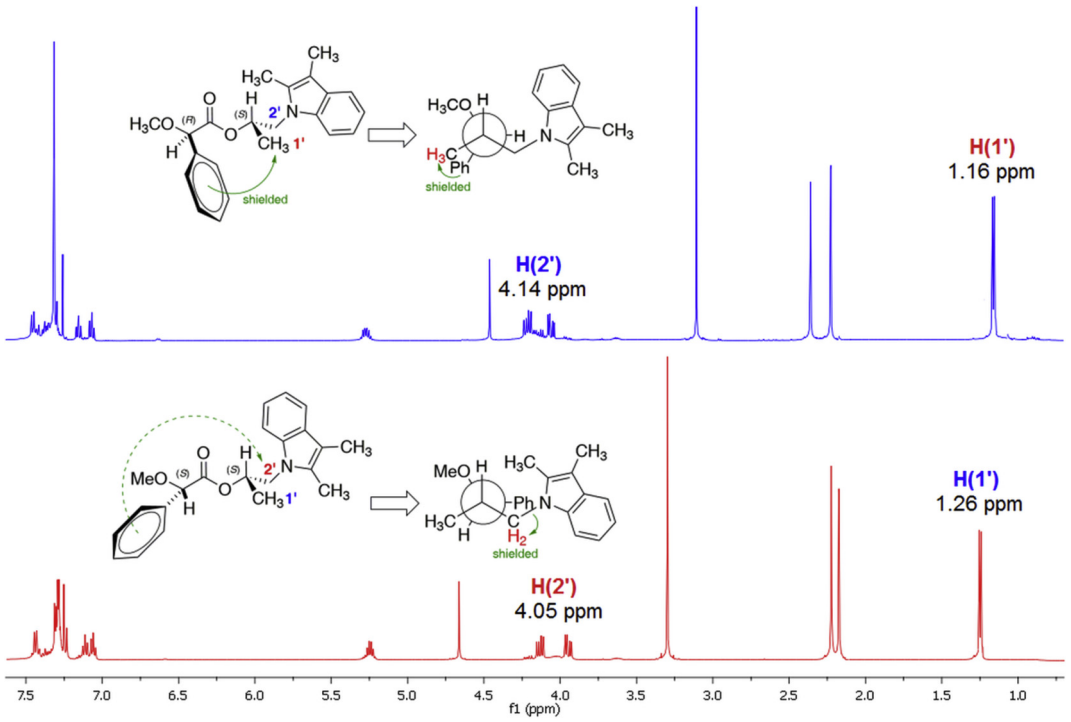

Figure 3. The ^{1}H NMR ($CDCl_3$, 500 MHz) spectra of the (*R*)-MPA (**6**, blue colored line) and (*S*)-MPA (**7**, red colored line) derivatives of chiral alcohol (+)-**3c**. Additionally, with red color are marked protons shielded by the phenyl ring of chiral auxiliary, blue labels stand for unaffected protons. Green arrows indicate the anisotropic shielding effect caused by the aromatic system. The ester carbonyl group is not shown in both the extended Newman projections for the sake of clarity.

type [(*S*)-(+)-**3c** and (*R*)-(−)-**4a**], it was clear that the stereochemical course of the performed enzymatic reactions is in agreement with Kazlauskas' empirical rule[62] regarding lipases' enantiopreference towards chiral *sec*-alcohols. In this context, the examined lipases favored faster transformation of (*R*)-alcohols over their antipodes. The same situation refers toward reversed reaction, in which the (*R*)-enantiomer of an ester was hydrolyzed at a faster rate than its (*S*)-counterpart.

3. Conclusion

Herein, an exploration of commercially available lipase preparations for enantioselective resolution of indole-based secondary alcohols and their respective esters has been reported for the first time. The enzymatic kinetic resolution methodology served as a model process, during which the reaction conditions were optimized with respect to enzyme screening, the organic solvent selection, and type of acyl group donor or acceptor, respectively. In this regard, three different approaches were compared: (i) lipase-catalyzed transesterification of racemic alcohols by means of enol esters (vinyl acetate and isopropenyl acetate), (ii) enzymatic hydrolysis, and (iii) enzymatic methanolysis of the target esters. By employing enzymatic kinetic resolution strategy both enantiomers of the studied racemates were accessible in enantiomerically pure form (>99% ee) or at least highly enantiomerically enriched. The most selective enzyme was lipase Amano AK from *Pseudomonas fluorescens* (up to $E \gg 400$). All of the enantiomeric compounds are potentially useful chiral intermediates for the synthesis of biologically active agents. To support the assignment of the absolute configurations of novel compounds a detailed ^{1}H NMR studies of Mosher esters as well as single-crystal XRD analysis were carried out appropriately.

4. Experimental section

4.1. Materials

Reagents and solvents were purchased from various commercial sources (Sigma Aldrich, Alfa Aesar, POCH) and were used without further purification. High-performance liquid chromatography (HPLC)-grade solvents were purchased from POCH (Poland). Methylene chloride and *N*,*N*-dimethylformamide were dried by allowing them to stand over activated (oven-roasted in high-vacuum) 3 Å molecular sieves [20% mass/volume (m/v) loading of the desiccant] at least for 48 h before use,[63] '*super-dry*' (absolute) toluene was prepared by simple passage thereof over a column of silica gel. All reactions, which needed anhydrous conditions (non-aqueous reactions), were carried out under an atmosphere of dry argon using flame-dried glasswares. Evaporation of the solvent residues was performed at reduced pressure by means of Büchi rotary evaporator. Lipase from *Candida antarctica B* (CAL-B) {Novozym 435—immobilized on the macroporous acrylic resin [poly (methyl methacrylate-co-butyl methacrylate)], specified activity: >10,000 U/g or 10 PLU/mg, water content 1.4%, and Lipozyme 435—immobilized on Lewatit VP OC 1600, both purchased from Novozymes A/S (Bagsvaerd, Denmark); and Chirazyme L-2, c.-f., C2, Lyo.—carrier-fixed on (carrier 2), specified activity: 150 kU, purchased from Roche}, lipase from *Thermomyces lanuginosus* (Lipozyme TL-IM-immobilized on silica gel (a silica granulated), specified activity: 170 IUN/g, purchased from Novozymes (Bagsvaerd, Denmark), lipase from *Burkholderia* (formerly *Pseudomonas*) *cepacia* [Amano PS—native lipase, specified activity: >23,000 U/g, purchased from Amano Pharmaceutical Co., Ltd], lipase from *Pseudomonas fluorescens* [Amano AK—native lipase, specified activity: >20,000 U/g, purchased from Amano Pharmaceutical Co., Ltd.], All commercial formulations of enzymes studied herein were used without any pretreatment.

4.2. Analytical methods

Melting points, uncorrected, were determined with a commercial apparatus on samples contained in rotating glass capillary tubes open on one side (1.35 mm inner diam. and 80 mm length). Analytical thin-layer chromatography was carried on TLC aluminum plates (Merck) covered with silica gel of 0.2 mm thickness film containing a fluorescence indicator green 254 nm (F_{254}), and using UV light as a visualizing agent. Preparative separations were carried out by: (i) column chromatography using thick-walled glass columns and silica gel (230–400 mesh) with grain size 40–63 μm or (ii) PLC PSC-Fertigplatten Kieselgel 60 F_{254} (20 × 20 cm with 2 mm thickness layer) glass plates purchased from Merck, Germany. The chromatographic analyses (GC) were performed with a Agilent Technologies 6850 instrument equipped with a flame ionization detector (FID) and fitted with HP-50+ (30 m) semipolar column (50% phenyl–50% methylpolysiloxane); helium (2 mL/min) was used as carrier gas; retention times (t_R) are given in minutes under these conditions. The enantiomeric excesses (% ee) of kinetic resolution products were determined by HPLC analysis performed on Shimadzu CTO-10ASV chromatograph equipped with STD-20A UV detector and Chiralcel OD-H chiral column (4.6 mm × 250 mm, from Daicel Chemical Ind., Ltd.) equipped with a pre-column (4 mm × 10 mm, 5 m) using mixtures of *n*-hexane/2-PrOH as mobile phase in the appropriate ratios given in experimental section [both the mobile phase composition as well as the flow rate were fine tuned for each analysis (see Table S1 in Supplementary data)]; the wavelength of UV detection was set at 254 nm; the HPLC analyses were executed in an isocratic and isothermal (30 °C) manner. Optical rotations ([α]) were measured with a PolAAr 32 polarimeter in a 2 dm long cuvette using the sodium D line (λ = 589 nm); the units of the specific rotation are: (deg × mL)/(g × dm). ^{1}H NMR (500 MHz) and ^{13}C NMR (126 MHz) spectra were recorded on a Varian NMR System 500 MHz spectrometer; ^{1}H and ^{13}C chemical shifts (δ) are reported in parts per million (ppm) relative to the solvent signals [$CDCl_3$, δ_H (residual $CHCl_3$) 7.26 ppm, δ_C 77.16 ppm]. Chemical shifts are quoted as s (singlet), d (doublet), dd (doublet of doublets), t (triplet), q (quartet), m (multiplet), and br s (broad singlet); coupling constants (*J*) are reported in Hertz. Mass spectrometry was recorded on Micro-mass ESI Q-TOF spectrometer [ESI, ESI-HRMS: additives of mixtures of MeCN/MeOH/H_2O (50:25:25, v/v) + 0.5% formic acid and MSI concept 1H (EI, 70eV ionization)].

4.3. Preparation of the racemic indole derivatives *rac*-3a–c

To a suspension of NaH (1.1 equiv, 60% mineral oil dispersion) in dry DMF (40 mL) the respective indole derivative **1a–c** (3 g) was added portionwise at 0–5 °C. Next, propylene oxide **2** (1.1 equiv) was added dropwise in a sufficient tempo not to increase the temperature over 0 °C. After the addition, stirring of the resultant suspension was continued for 24 h at room temperature. The content of the flask was poured over H_2O (80 mL), and the separated aqueous solution was extracted with EtOAc (3 × 15 mL). The combined organic layer was dried over anhydrous $MgSO_4$, then the drying agent was filtered off, and the volatiles were removed under reduced pressure. The resultant crude mixture was further high-vacuum-dried in order to remove the residual DMF, and subsequently purified by column chromatography on SiO_2 using mixture of *n*-hexane/EtOAc in various volume ratios depending on the reaction, thus yielding the corresponding racemic alcohols *rac*-**3a–c**.

4.3.1. 1-(5-Nitro-1*H*-indol-1-yl)propan-2-ol *rac*-3a

Purified using 50% EtOAc/*n*-hexane as an eluent; yield 43% (1.75 g); yellow solid; mp 101–103 °C (*n*-hexane/EtOAc); ^{1}H NMR (500 MHz, $CDCl_3$): δ 1.28 (d, J = 6.4 Hz, 3H), 1.80 (br s, 1H), 4.01–4.13 (m, 1H), 4.14–4.28 (m, 2H), 6.55–6.74 (m, 1H), 7.28–7.32 (m, 1H), 7.33–7.44 (m, 1H), 7.97–8.13 (m, 1H), 8.45–8.58 (m, 1H); ^{13}C NMR (126 MHz, $CDCl_3$): δ 20.8, 53.9, 67.3, 104.2, 109.5, 117.3, 118.2, 127.7, 131.9, 139.3, 141.5; HRMS (ESI-TOF) m/z: $[M+H]^+$ Calcd for $C_{11}H_{13}N_2O_3^+$ 221.0926, Found 221.0833; GC [150–260 (10 °C/min)]: t_R = 12.12 min or [100–260 (2 °C/min)]: t_R = 60.49 min; HPLC [5% 2-PrOH/*n*-hexane; f = 0.8 mL/min; λ = 254 nm]: t_R = 46.03 (*S*-isomer) and 53.32 min (*R*-isomer).

4.3.2. 1-(3-Methyl-1*H*-indol-1-yl)propan-2-ol *rac*-3b

Purified using 29% EtOAc/*n*-hexane as an eluent; yield 56% (2.43 g); green oil; ^{1}H NMR (500 MHz, $CDCl_3$): δ 1.26 (d, J = 6.4, 3H), 1.70 (br s, 1H), 2.33 (d, J = 1.0, 3H), 3.93–4.01 (m, 1H), 4.07–4.14 (m, 1H), 4.14–4.23 (m, 1H), 6.87–6.96 (m, 1H), 7.09–7.16 (m, 1H), 7.19–7.25 (m, 1H), 7.30–7.36 (m, 1H), 7.55–7.62 (m, 1H); ^{13}C NMR (126 MHz, $CDCl_3$): δ 9.5, 20.4, 53.6, 67.4, 109.3, 110.0, 110.8, 118.8, 119.1, 121.6, 126.0, 136.6; HRMS (ESI-TOF) m/z: $[M+H]^+$ Calcd for $C_{12}H_{16}NO^+$ 190.1232, Found 190.1231; GC [150–260 (10 °C/min)]: t_R = 6.53 min; HPLC [5% 2-PrOH/*n*-hexane; f = 0.7 mL/min; λ = 254 nm]: t_R = 18.69 (*S*-isomer) and 21.31 min (*R*-isomer).

4.3.3. 1-(2,3-Dimethyl-1*H*-indol-1-yl)propan-2-ol *rac*-3c

Purified using 60% EtOAc/*n*-hexane as an eluent; yield 70% (2.95 g); yellowish oil; ^{1}H NMR (500 MHz, $CDCl_3$): δ ppm 1.29 (d, J = 6.4 Hz, 3H), 1.65 (br s, 1H), 2.26 (s, 3H), 2.38 (s, 3H), 3.95–4.10 (m, 2H), 4.13–4.26 (m, 1H), 7.02–7.19 (m, 2H), 7.22–7.35 (m, 1H), 7.44–7.56 (m, 1H); ^{13}C NMR (126 MHz, $CDCl_3$): δ 8.8, 10.5, 20.5, 50.8, 67.4, 107.0, 108.9, 110.0, 118.0, 118.9, 120.7, 128.7, 136.2; HRMS (ESI-TOF) m/z: $[M+H]^+$ Calcd for $C_{13}H_{18}NO^+$ 204.1388, Found 204.1365; GC [150–260 (10 °C/min)]: t_R = 7.32 min; HPLC [4% 2-PrOH/*n*-hexane; f = 0.4 mL/min; λ = 254 nm]: t_R = 26.59 (*S*-isomer) and 29.35 min (*R*-isomer).

4.4. Preparation of the racemic indole acetates *rac*-4a–c

To the solution of the appropriate racemic alcohol *rac*-**3a**–**c** (1 g) in dry CH_2Cl_2 (20 mL), acetic anhydride (1.1 equiv) and a catalytic amount of DMAP (15 mg) were added in one portion. The resulting reaction mixture was stirred at room temperature for 24 h, and then quenched with saturated $NaHCO_3$ solution (3 × 20 mL), and H_2O (20 mL). The water phase was extracted with CH_2Cl_2 (3 × 50 mL), the combined organic layers were washed with aqueous $NaHCO_3$ (100 mL), and then dried over anhydrous $MgSO_4$. After solvent removal under reduced pressure, the crude product was passed through short column chromatography on silica gel using a mixture of *n*-hexane/EtOAc in various volume ratios depending on the reaction, thus yielding the corresponding racemic acetate *rac*-**4a**–**c**, respectively.

4.4.1. 1-(5-Nitro-1*H*-indol-1-yl)propan-2-yl acetate *rac*-4a

Purified using 50% EtOAc/*n*-hexane as an eluent; yield 85% (1.01 g); yellow solid; mp 58.5–59 °C (*n*-hexane/EtOAc); ^{1}H NMR (500 MHz, $CDCl_3$): δ 1.27 (d, J = 6.4 Hz, 3H), 1.93 (s, 3H), 4.18–4.25 (m, 1H), 4.27–4.35 (m, 1H), 5.16–5.33 (m, 1H), 6.65–6.73 (m, 1H), 7.21–7.25 (m, 1H), 7.36–7.48 (m, 1H), 8.04–8.17 (m, 1H), 8.49–8.63 (m, 1H); ^{13}C NMR (126 MHz, $CDCl_3$): δ 17.7, 21.0, 50.9, 69.3, 104.5, 109.5, 117.4, 118.2, 127.7, 131.4, 139.3, 141.7, 170.1; HRMS (ESI-TOF) m/z: $[M+H]^+$ Calcd for $C_{13}H_{15}N_2O_4^+$ 263.1032, Found 263.1089; GC [100–260 (2 °C/min)]: t_R = 61.34 min; HPLC [5% 2-PrOH/*n*-hexane; f = 0.8 mL/min; λ = 254 nm]: t_R = 34.83 (*S*-isomer) and 36.74 min (*R*-isomer).

4.4.2. 1-(3-Methyl-1*H*-indol-1-yl)propan-2-yl acetate *rac*-4b

Purified using 29% EtOAc/*n*-hexane as an eluent; yield 85% (1.04 g); yellowish oil; ^{1}H NMR (500 MHz, $CDCl_3$): δ ppm 1.23 (d, J = 6.4 Hz, 3H), 1.98 (s, 3H), 2.32 (d, J = 1.0 Hz, 3H), 4.08 (dd, J = 14.7, 5.4 Hz, 1H), 4.22 (dd, J = 14.7, 6.4 Hz, 1H), 5.18–5.27 (m, 1H), 6.83–6.88 (m, 1H), 7.08–7.14 (m, 1H), 7.19–7.24 (m, 1H), 7.33–7.38 (d, J = 8.3 Hz, 1H), 7.53–7.59 (m, 1H); ^{13}C NMR (126 MHz, $CDCl_3$): δ 9.6, 17.7, 21.2, 50.1, 69.8, 109.3, 110.9, 118.8, 119.0, 121.6, 125.8, 128.7, 136.8, 170.3; HRMS (ESI-TOF) m/z: $[M+H]^+$ Calcd for $C_{14}H_{18}NO_2^+$ 232.1338, Found 232.1242; GC [150–260 (10 °C/min)]: t_R = 7.15 min; HPLC [5% 2-PrOH/*n*-hexane; f = 0.7 mL/min; λ = 254 nm]: t_R = 13.61 (*S*-isomer) and 14.96 min (*R*-isomer).

4.4.3. 1-(2,3-Dimethyl-1*H*-indol-1-yl)propan-2-yl acetate *rac*-4c

Purified using 60% EtOAc/*n*-hexane as an eluent; yield 78% (941 mg); yellowish oil; ^{1}H NMR (500 MHz, $CDCl_3$): δ ppm 1.28 (d, J = 6.4 Hz, 3H), 1.95 (s, 3H), 2.27 (s, 3H), 2.40 (s, 3H), 4.06 (dd, J = 14.9, 5.6 Hz, 1H), 4.24 (dd, J = 14.9, 7.1 Hz, 1H), 5.24 (dd, J = 12.7, 6.4 Hz, 1H), 7.07–7.13 (m, 1H), 7.14–7.20 (m, 1H), 7.30–7.36 (m, 1H), 7.47–7.52 (m, 1H); ^{13}C NMR (126 MHz, $CDCl_3$): δ 8.9, 10.3, 17.9, 21.1, 47.3, 69.7, 107.1, 109.0, 117.9, 118.9, 120.7, 128.6, 132.2, 136.4, 170.2; HRMS (ESI-TOF) m/z: $[M+H]^+$ Calcd for $C_{15}H_{20}NO_2^+$ 246.1494, Found 246.1419; GC [150–260 (10 °C/min)]: t_R = 7.81 min; HPLC [4% 2-PrOH/*n*-hexane; f = 0.4 mL/min; λ = 254 nm]: t_R = 12.38 (*S*-isomer) and 13.43 min (*R*-isomer).

4.5. Preparation of the racemic indole butyrates *rac*-5a–c

To a solution of the appropriate racemic alcohol *rac*-**3a**–**c** (600 mg) in dry $PhCH_3$ (10 mL), Et_3N (1 equiv) and catalytic amount of DMAP (15 mg) were added. Next, butyryl chloride (1 mmol) was dissolved in dry $PhCH_3$ (2 mL), and subsequently added to the reaction mixture in a dropwise manner at 0–5 °C. The content of the flask was warmed to room temperature, and stirred at room temperature for 24 h. After this time, the crude mixture was quenched with H_2O (20 mL), the water phase was extracted with EtOAc (3 × 10 mL), and the combined organic layer was washed with saturated aqueous solution of $NaHCO_3$ (50 mL), brine (50 mL), and dried over anhydrous $MgSO_4$. After evaporation of the residuals of solvent, the crude product was purified by column chromatography on silica gel using mixture of *n*-hexane/EtOAc in various volume ratios depending on the reaction, thus obtaining desire butyrate *rac*-**4a**–**c**, respectively.

4.5.1. 1-(5-Nitro-1*H*-indol-1-yl)propan-2-yl butyrate *rac*-5a

Purified using 50% EtOAc/*n*-hexane as an eluent; yield 73% (580 mg); brownish solid; mp 78–83 °C (*n*-hexane/EtOAc); ^{1}H NMR (500 MHz, $CDCl_3$): δ 0.81 (t, J = 7.3 Hz, 3H), 1.28 (d, J = 6.4 Hz, 3H), 1.51 (sxt, J = 7.4 Hz, 2H), 2.05–2.27 (m, 2H), 4.16–4.25 (m, 1H), 4.26–4.36 (m, 1H), 5.13–5.41 (m, 1H), 6.62–6.75 (m, 1H), 7.21–7.25 (m, 1H), 7.37–7.49 (m, 1H), 8.07–8.18 (m, 1H), 8.52–8.61 (m, 1H); ^{13}C NMR (126 MHz, $CDCl_3$): δ 13.4, 17.7, 18.2, 36.1, 50.9, 69.0, 104.5, 109.5, 117.4, 118.2, 127.7, 131.4, 139.3, 141.7, 172.7; HRMS (ESI-TOF) m/z: $[M+H]^+$ Calcd for $C_{15}H_{19}N_2O_4^+$ 291.1345, Found 291.1163; GC [150–260 (10 °C/min)]: t_R = 13.99 min; HPLC [5% 2-PrOH/*n*-hexane; f = 0.8 mL/min; λ = 254 nm]: t_R = 24.25 (*S*-isomer) and 26.48 min (*R*-isomer).

4.5.2. 1-(3-Methyl-1*H*-indol-1-yl)propan-2-yl butyrate *rac*-5b

Purified using 60% EtOAc/*n*-hexane as an eluent; yield 65% (535 mg); yellowish oil; ^{1}H NMR (500 MHz, $CDCl_3$): δ 0.89 (t, J = 7.3 Hz, 3H) 1.25 (d, J = 6.4 Hz, 3H), 1.52–1.70 (m, 2H), 2.15–2.29 (m, 2H), 2.34 (s, 3H), 4.09 (dd, J = 14.7, 5.4 Hz, 1H), 4.24 (dd, J = 14.9, 6.6 Hz, 1H), 5.25 (dq, J = 12.3, 6.2 Hz, 1H), 6.87 (s, 1H), 7.05–7.18 (m, 1H), 7.19–7.29 (m, 1H), 7.32–7.44 (m, 1H), 7.51–7.65 (m, 1H);

^{13}C NMR (126 MHz, $CDCl_3$): δ 9.6, 13.5, 17.8, 18.3, 36.3, 50.1, 69.5, 109.3, 110.9, 118.8, 119.0, 121.6, 125.9, 128.7, 136.8, 173.0; HRMS (ESI-TOF) *m*/*z*: $[M+H]^+$ Calcd for $C_{16}H_{22}NO_2^+$ 260.1651, Found 260.1143; GC [150–260 (10 °C/min)]: t_R = 8.06 min.

4.5.3. 1-(2,3-Dimethyl-1*H*-indol-1-yl)propan-2-yl butyrate *rac*-5c

Purified using 60% EtOAc/*n*-hexane as an eluent; yield 62% (502 mg); brown oil; ^{1}H NMR (500 MHz, $CDCl_3$): δ 0.83 (t, *J* = 7.6 Hz, 3H), 1.25 (d, *J* = 6.4 Hz, 3H), 1.52 (dqd, *J* = 14.8, 7.5, 7.5, 7.5, 2.0 Hz, 2H), 2.08–2.22 (m, 2H), 2.24 (s, 3H), 2.38 (s, 3H), 4.01–4.09 (m, 1H), 4.23 (dd, *J* = 15.2, 7.3 Hz, 1H), 5.24 (dq, *J* = 13.1, 6.4 Hz, 1H), 7.03–7.19 (m, 2H), 7.29–7.37 (m, 1H), 7.44–7.50 (m, 1H); ^{13}C NMR (126 MHz, $CDCl_3$): δ 8.8, 10.3, 13.5, 17.9, 18.2, 36.2, 47.3, 69.4, 107.1, 109.0, 117.9, 118.8, 120.7, 128.6, 132.1, 136.4, 172.9; HRMS (ESI-TOF) *m*/*z*: $[M+H]^+$ Calcd for $C_{17}H_{24}NO_2^+$ 274.1807, Found 274.1528; GC [150–260 (10 °C/min)]: t_R = 9.12 min.

4.6. Enzymatic kinetic resolution studies

4.6.1. General procedure for lipase-catalyzed enantioselective hydrolysis/methanolysis of *rac*-4a–b and *rac*-5a under kinetically-controlled conditions

To a solution of *rac*-**4a** or *rac*-**4b** or *rac*-**5a** (50 mg) in water-saturated TBME (3 mL) or a mixture of organic solvent (3 mL) and methanol (10 equiv), the respective lipase preparation [5 mg, 10% w/w (catalyst/substrate)] was added, and the reaction mixture was shaken (300 rpm) with incubation at 30 °C by using a laboratory rotatory shaker. After the necessary time to achieve good kinetic resolution (see Tables 1 and 4), the biotransformation process was terminated by enzyme removal and subsequent washing with the appropriate solvent (1.5 mL). For hydrolytic attempts, the permeate was additionally dried over Na_2SO_4, filtered off, and evaporated to dryness under reduced pressure, and only then purified by column chromatography. For enzymatic methanolysis, after enzyme removal the concentrated crude residue was directly subjected to column chromatography on silica gel using mixture of 50% EtOAc/*n*-hexane as the eluent yielding optically active products [acetates (*S*)-(+)-**4a**–**b** or butyrate (*S*)-(+)-**5a**, and alcohol (*R*)-(−)-**3a**] in yields >90% (referred to the corresponding conversion value). For the most enantiomerically pure resolution products, the specific rotations were measured, and are as follows: (*S*)-(+)-**4a**: $[\alpha]_D^{25}$ = +8.3 (*c* 0.30, CH_2Cl_2, >99% ee); (*R*)-(−)-**3a**: $[\alpha]_D^{25}$ = −20.7 (*c* 0.29, CH_2Cl_2, 99% ee).

4.6.2. General procedure for lipase-catalyzed enantioselective transesterification of *rac*-3a–c under kinetically-controlled conditions

To a solution of the appropriate racemic indole-like alcohol *rac*-**3a**–**c** (50 mg) in the respective organic solvent (3 mL), lipase preparation [5 mg, 10% w/w (catalyst/substrate)] and vinyl acetate (10 equiv) or isopropenyl acetate (10 equiv) were added in one portion. Thus composed reaction mixture was shaken (300 rpm) at 30 °C by using a laboratory rotatory shaker, while its aliquots were regularly analyzed by analytical chromatographic assays (GC and HPLC). When the appropriate conversion was reached, the reaction was terminated by filtering off the enzyme on a Schott funnel, and by subsequent washing it with corresponding organic solvent (2 × 5 mL). The permeate was concentrated under reduced pressure, and the crude residue was purified by column chromatography on silica gel using a binary solvent system composed of mixture of 50% EtOAc/*n*-hexane for kinetic resolution of *rac*-**3a**, 60% EtOAc/*n*-hexane for kinetic resolution of *rac*-**3b**, and 50% EtOAc/*n*-hexane for kinetic resolution of *rac*-**3c**. The respective resolution products [(*R*)-(−)-**3a**–**c** and (*S*)-(+)-**4a**–**c**] were isolated in yields >90% (referred to the corresponding conversion value), and fully characterized in terms of spectroscopic and optical properties. The detailed experimental conditions, and the results of enzymatic kinetic resolution reactions (including enantiomeric excess data for the resolved products and values of enantioselectivity factor) are collected in Tables: 2, 3, and 6–8. The specific rotations for the enantiomerically enriched esters (*R*)-(−)-**4a**–**c** and alcohols (*S*)-(+)-**3a**–**c** are as follows: (*S*)-(+)-**3a**: $[\alpha]_D^{25}$ = +12.3 (*c* 0.54, CH_2Cl_2, >99% ee); (*R*)-(−)-**4a**: $[\alpha]_D^{25}$ = −8.6 (*c* 0.46, CH_2Cl_2, >99% ee); (*S*)-(+)-**3b**: $[\alpha]_D^{25}$ = +14.5 (*c* 1.0, CH_2Cl_2, 87% ee); (*R*)-(−)-**4b**: $[\alpha]_D^{25}$ = −10.0 (*c* 1.0, CH_2Cl_2, 98% ee); (*S*)-(+)-**3c**: $[\alpha]_D^{25}$ = +10.3 (*c* 0.82, CH_2Cl_2, >99% ee); (*R*)-(−)-**4c**: $[\alpha]_D^{25}$ = −6.8 (*c* 1.02, CH_2Cl_2, 99% ee).

4.7. Determination of the absolute configuration of (*S*)-(+)-3c

4.7.1. Esterification of (*S*)-(+)-1-(2,3-dimethyl-1*H*-indol-1-yl) propan-2-ol (*S*)-(+)-3c with (*R*)- or (*S*)-α-methoxy-α-phenylacetic acid

A solution of enantiopure indole-like alcohol (*S*)-(+)-**3c** (13.3 mg, 0.07 mmol, >99% ee), (*R*)- or (*S*)-α-methoxy-α-phenylacetic acid (10.9 mg, 0.07 mmol) as appropriate, DCC (16.2 mg, 0.07 mmol) and DMAP (15 mg) in anhydrous CH_2Cl_2 (4 mL) was stirred for 3 h at room temperature. Next, the precipitated dicyclohexylurea (DCU) was removed by filtration, and the urea cake was rinsed with CH_2Cl_2 (10 mL). The combined CH_2Cl_2 solutions were washed with saturated $NaHCO_3$ (3 × 10 mL) and H_2O (10 mL), dried over anhydrous $MgSO_4$, and after filtration of the drying agent evaporated in vacuum. The crude product was purified by preparative layer chromatography using a mixture of 50% EtOAc/*n*-hexane as an eluent to afford the corresponding products **6** or **7** as yellowish oils.

4.7.1.1. (*R*)-MPA ester 6. Yield = 85%; ^{1}H NMR (500 MHz, $CDCl_3$) δ: 1.16 (d, *J* = 6.4 Hz, 3H), 2.23 (s, 3H), 2.36 (s, 3H), 3.11 (s, 3H), 4.06 (dd, *J* = 14.9, 5.1 Hz, 1H), 4.22 (dd, *J* = 15.2, 8.2 Hz, 1H), 4.46 (s, 1H), 5.17–5.37 (m, 1H), 7.02–7.51 (m, 9H).

4.7.1.2. (*S*)-MPA ester 7. Yield = 82%; ^{1}H NMR (500 MHz, $CDCl_3$) δ: 1.26 (d, *J* = 6.4 Hz, 3H), 2.18 (s, 3H), 2.23 (s, 3H), 3.31 (s, 3H), 3.95 (dd, *J* = 15.2, 5.9 Hz, 1H), 4.14 (dd, *J* = 15.2, 7.3 Hz, 1H), 4.67 (s, 1H), 5.20–5.30 (m, 1H), 7.04–7.17 (m, 2H), 7.22–7.48 (m, 7H).

4.8. X-ray structure determination

In order to produce single crystals suitable for X-ray diffraction analysis, enantiomerically pure (*R*)-(−)-**4a** (20 mg, >99% ee) was dissolved in *n*-hexane (1 mL) at reflux. Next, EtOAc (0.5 mL) was carefully added, and the solution was rapidly cooled down to room temperature to initiate nucleation under stagnant conditions. The system was stored at room temperature, and crystal growth was allowed to proceed overnight with slow evaporation of the solvents. The crystals were selected under Paratone-N oil, mounted on the nylon loops and positioned in the cold stream on the diffractometer. The X-ray data for (*R*)-(−)-**4a** was collected at 100(2) K on a SuperNova Agilent diffractometer using CuKα radiation (λ = 1.54184 Å). The data were processed with *CrysAlisPro*.[64] The structure was solved by direct methods using the SHELXS-97 program and was refined by full matrix least-squares on F^2 using the program SHELXL-97.[65] All non-hydrogen atoms were refined with anisotropic displacement parameters. Hydrogen atoms were added to the structure model at geometrically idealized coordinates and refined as riding atoms. Crystallographic data (excluding structure factors) for the structure reported in this paper have been deposited with the Cambridge Crystallographic Data Centre as supple-

mentary publication. Copies of the data can be obtained free of charge on application to CCDC, 12 Union Road, Cambridge CB21EZ, UK (fax: (+44)1223-336-033; e-mail: deposit@ccdc.cam.ac.uk).

Crystal data for (*R*)-(−)-**4a**; $C_{13}H_{14}N_2O_4$: M = 262.26, crystal dimensions 0.32 × 0.24 × 0.12 mm^3, triclinic, space group $P\bar{1}$ (no. 2), a = 4.69080(10) Å, b = 10.7522(3) Å, c = 12.3836(4) Å, β = 87.214(2), U = 624.58(3) Å^3, Z = 2, $F(000)$ = 276, D_c = 1.395 g cm^{-3}, T = 100(2) K, μ(Mo-Kα) = 0.877 mm^{-1}, SuperNova Agilent diffractometer, θ_{max} = 69.482°, $R1$ = 0.0302, $wR2$ = 0.0782 for all data, $R1$ = 0.0299, $wR2$ = 0.0779 for 2197 reflections with $I_o > 2\sigma(I_o)$. The goodness-of-fit on F^2 was equal 1.064. A weighting scheme $w = [\sigma^2(F_o^2) + (0.0418P)^2 + 3.1964P]^{-1}$ where $P = (F_o^2 + 2F_c^2)/3$ was used in the final stage of refinement. The residual electron density = +0.15/−0.19 eÅ^{-3}. CCDC—1500811.

Acknowledgements

This work was financially supported by Warsaw University of Technology (Faculty of Chemistry) in the frame of '*Dean's Funding Program for Young Investigators*'. The authors wish to gratefully acknowledge Prof. Jan Plenkiewicz for proof-reading and critical opinions helpful for preparing this manuscript. In addition, we would like to extend our sincere gratitude and appreciation for all of the hard work and dedication provided by undergraduate students: Maryia Sheiherevich, Anna Stolarczyk, and Katarzyna Banasik.

A. Supplementary data

Supplementary data associated with this article can be found, in the online version, at https://doi.org/10.1016/j.tetasy.2017.10.010.

References

1. (a) Fischer, E.; Jourdan, F. *Ber. Deut. Chem. Gesell.* **1883**, *16*, 2241–2245; (b) Fischer, E.; Hess, O. *Ber. Deut. Chem. Gesell.* **1884**, *17*, 559–568; (c) Fischer, E. *Chem. Ber.* **1886**, *19*, 1547–1567; (d) Fischer, E. *Liebigs Ann. Chem.* **1886**, *236*, 141–142.
2. (a) Houlihan, W. J. *Chemistry of Heterocyclic Compounds: Indoles, Part One*; John Wiley & Sons, 1971; p 25; (b) Robinson, B. *The Fischer Indole Synthesis*; Wiley-Interscience: New York, 1982.
3. (a) Gribble, G. W. *J. Chem. Soc., Perkin Trans. 1* **2000**, 1045–1075; (b) Humphrey, G. R.; Kuethe, J. T. *Chem. Rev.* **2006**, *106*, 2875–2911; (c) Vicente, R. *Org. Biomol. Chem.* **2011**, *9*, 6469–6480; (d) Taber, D. F.; Tirunahari, P. K. *Tetrahedron* **2011**, *67*, 7195–7210; (e) Inman, M.; Moody, C. *J. Chem. Sci.* **2013**, *4*, 29–41; (f) Bartoli, G.; Dalpozzo, R.; Nardi, M. *Chem. Soc. Rev.* **2014**, *43*, 4728–4750; (g) Marelli, E.; Corpet, M.; Minenkov, Y.; Neyyappadath, R. M.; Bismuto, A.; Buccolini, G.; Curcio, M.; Cavallo, L.; Nolan, S. P. *ACS Catal.* **2016**, *6*, 2930–2938; (h) Choi, I.; Chung, H.; Park, J. W.; Chung, Y. K. *Org. Lett.* **2016**, *18*, 5508–5511; (i) Garcia-Munoz, M. J.; Foubelo, F.; Yus, M. *J. Org. Chem.* **2016**, *81*, 10214–10226.
4. (a) Cacchi, S.; Fabrizi, G. *Chem. Rev.* **2005**, *105*, 2873–2920; (b) Bartoli, G.; Bencivenni, G.; Dalpozzo, R. *Chem. Soc. Rev.* **2010**, *39*, 4449–4465; (c) Cacchi, S.; Fabrizi, G. *Chem. Rev.* **2011**, *111*, 3; (d) Shiri, M. *Chem. Rev.* **2012**, *112*, 3508–3549; (e) Dalpozzo, R. *Chem. Soc. Rev.* **2015**, *44*, 742–778; (f) Bertuzzi, G.; Sinisi, A.; Caruana, L.; Mazzanti, A.; Fochi, M.; Bernardi, L. *ACS Catal.* **2016**, *6*, 6473–6477; (g) Jiang, L.; Jin, W.; Hu, W. *ACS Catal.* **2016**, *6*, 6146–6150; (h) Fischereder, E.-M.; Pressnitz, D.; Kroutil, W. *ACS Catal.* **2016**, *6*, 23–30.
5. (a) Rahman, A. *Indole Alkaloids*; Harwood Academic Publisher: Amsterdam, 1998; (b) Takayama, H. *Chem. Pharm. Bull.* **2004**, *52*, 916–928; (c) Mizoguchi, H.; Oikawa, H.; Oguri, H. *Nat. Chem.* **2014**, *6*, 57–64.
6. (a) Aygun, A.; Pindur, U. *Curr. Med. Chem.* **2003**, *10*, 1113–1127; (b) Gul, W.; Hamann, M. T. *Life Sci.* **2005**, *78*, 442–453; (c) Gupta, L.; Talwar, A.; Chauhan, M. S. *Curr. Med. Chem.* **2007**, *14*, 1789–1803; (d) Kochanowska-Karamyan, A. J.; Hamann, M. T. *Chem. Rev.* **2010**, *110*, 4489–4497; (e) Manda, S.; Sharma, S.; Wani, A.; Joshi, P.; Kumar, V.; Guru, S. K.; Bharate, S. S.; Bhushan, S.; Vishwakarma, R. A.; Kumar, A.; Bharate, S. B. *Eur. J. Med. Chem.* **2016**, *107*, 1–11.
7. (a) Xu, W.; Gavia, D. J.; Tang, Y. *Nat. Prod. Rep.* **2014**, *31*, 1474–1487; (b) Adams, T. C.; Payette, J. N.; Cheah, J. H.; Movassaghi, M. *Org. Lett.* **2015**, *17*, 4268–4271; (c) Motoyama, T.; Osada, H. *Bioorg. Med. Chem. Lett.* **2016**, *26*, 5843–5850.
8. (a) Bush, J. A.; Long, B. H.; Catino, J. J.; Bradner, W. T. *J. Antibiot.* **1987**, *40*, 668–678; (b) Nishizawa, T.; Gruschow, S.; Jayamaha, D. H.; Nishizawa-Harada, C.; Sherman, D. H. *J. Am. Chem. Soc.* **2006**, *128*, 724–725; (c) Marsch, N.; Jones, P. G.; Lindel, T. *Beilstein J. Org. Chem.* **2015**, *11*, 1700–1706.
9. (a) Newhouse, T.; Lewis, C. A.; Eastman, K. J.; Baran, P. S. *J. Am. Chem. Soc.* **2010**, *132*, 7119–7137; (b) Adla, S. K.; Sasse, F.; Kelter, G.; Fiebig, H. H.; Lindel, T. *Org. Biomol. Chem.* **2013**, *11*, 6119–6130; (c) Lancianesi, S.; Palmieri, A.; Petrini, M. *Chem. Rev.* **2014**, *114*, 7108–7149.
10. (a) de Sa Alves, F.; Barreiro, E.; Manssour Fraga, C. *Mini-Rev. Med. Chem.* **2009**, *9*, 782–793; (b) Bronner, S. M.; Im, G. Y. J.; Garg, N. K. Heterocycles in Natural Product Synthesis *Wiley-VCH* **2011**, 221–265; (c) Biswal, S.; Sahoo, U.; Sethy, S.; Kumar, H. K. S.; Banerjee, M. *Asian J. Pharm. Clin. Res.* **2012**, *5*, 1–6; (d) Sravanthi, T. V.; Manju, S. L. *Eur. J. Pharm. Sci.* **2016**, *91*, 1–10.
11. (a) Dydio, P.; Ploeger, M.; Reek, J. N. H. *ACS Catal.* **2013**, *3*, 2939–2942; (b) Dydio, P.; Detz, R. J.; de Bruin, B.; Reek, J. N. H. *J. Am. Chem. Soc.* **2014**, *136*, 8418–8429; (c) Dydio, P.; Reek, J. N. H. *Nat. Prot.* **2014**, *9*, 1183–1191; (d) Chen, T.; Foo, T. J. Y.; Yeung, Y.-Y. *ACS Catal.* **2015**, *5*, 4751–4755; (e) Théveau, L.; Bellini, R.; Dydio, P.; Szabo, Z.; van der Werf, A.; Afshin Sander, R.; Reek, J. N. H.; Moberg, C. *Organometallics* **2016**, *35*, 1956–1963.
12. (a) Zollinger, H. *Color Chemistry: Syntheses, Properties and Applications of Organic Dyes And Pigments*, 3rd ed.; Wiley-VCH: Weinheim, 2003; (b)*Industrial Dyes: Chemistry, Properties, Applications*; Hunger, K., Ed.; Wiley-VCH: New York, 2003.
13. Barden, T. C. *Top. Heterocycl. Chem.* **2010**, *26*, 31–46.
14. Kondo, Y.; Fukuda, K.; Makabe, T.; Kondo, Y.; Fukuda, K.; Sakurai, Y.; Utsunomiya, T. *Processes for Production of Indole Compounds*. Patent EP1829872, **2007**.
15. (a) Berger, L.; Corraz A. J. Carbazoles. Patent US3896145, **1975**.; (b) Vigano', E.; Colombo, P. *Process for the Preparation of Etodolac*. Patent US6066741A, **2000**.
16. Flachsmann, F.; Bachmann, J. -P. *Organic compounds*. Patent US 20090036690 A1, **2009**.
17. Martins, P.; Jesus, J.; Santos, S.; Raposo, L. R.; Roma-Rodrigues, C.; Baptista, P. V.; Fernandes, A. R. *Molecules* **2015**, *20*, 16852–16891.
18. (a) Bai, J.; Liao, C.; Liu, Y.; Qin, X.; Chen, J.; Qiu, Y.; Qin, D.; Li, Z.; Tu, Z.-C.; Jiang, S. *J. Med. Chem.* **2016**, *59*, 5766–5779; (b) Daniele, S.; La Pietra, V.; Barresi, E.; Di Maro, S.; Da Pozzo, E.; Robello, M.; La Motta, C.; Cosconati, S.; Taliani, S.; Marinelli, L.; Novellino, E.; Martini, C.; Da Settimo, F. *J. Med. Chem.* **2016**, *59*, 4526–4538; (c) Fortes, M. P.; da Silva, P. B. N.; da Silva, T. G.; Kaufman, T. S.; Militão, G. C. G.; Silveira, C. C. *Eur. J. Med. Chem.* **2016**, *118*, 21–26; (d) Mahal, K.; Biersack, B.; Schruefer, S.; Resch, M.; Ficner, R.; Schobert, R.; Mueller, T. *Eur. J. Med. Chem.* **2016**, *118*, 9–20; (e) Pelz, N. F.; Bian, Z.; Zhao, B.; Shaw, S.; Tarr, J. C.; Belmar, J.; Gregg, C.; Camper, D. V.; Goodwin, C. M.; Arnold, A. L.; Sensintaffar, J. L.; Friberg, A.; Rossanese, O. W.; Lee, T.; Olejniczak, E. T.; Fesik, S. W. *J. Med. Chem.* **2016**, *59*, 2054–2066; (f) Spindler, A.; Stefan, K.; Wiese, M. *J. Med. Chem.* **2016**, *59*, 6121–6135; (g) Vaswani, R. G.; Gehling, V. S.; Dakin, L. A.; Cook, A. S.; Nasveschuk, C. G.; Duplessis, M.; Iyer, P.; Balasubramanian, S.; Zhao, F.; Good, A. C.; Campbell, R.; Lee, C.; Cantone, N.; Cummings, R. T.; Normant, E.; Bellon, S. F.; Albrecht, B. K.; Harmange, J.-C.; Trojer, P.; Audia, J. E.; Zhang, Y.; Justin, N.; Chen, S.; Wilson, J. R.; Gamblin, S. J. *J. Med. Chem.* **2016**, *59*, 9928–9941; (h) Yan, J.; Chen, J.; Zhang, S.; Hu, J.; Huang, L.; Li, X. *J. Med. Chem.* **2016**, *59*, 5264–5283; (i) Zhang, C.; Qu, Y.; Niu, B. *Bioorg. Med. Chem.* **2016**, *24*, 5781–5786; (j) Boraei, A. T. A.; Gomaa, M. S.; El Ashry, E. S. H.; Duerkop, A. *Eur. J. Med. Chem.* **2017**, *125*, 360–371; (k) Yan, J.; Hu, J.; An, B.; Huang, L.; Li, X. *Eur. J. Med. Chem.* **2017**, *125*, 663–675.
19. (a) Sosič, I.; Anderluh, M.; Sova, M.; Gobec, M.; Mlinarič Raščan, I.; Derouaux, A.; Amoroso, A.; Terrak, M.; Breukink, E.; Gobec, S. *J. Med. Chem.* **2015**, *58*, 9712–9721; (b) Lepri, S.; Buonerba, F.; Goracci, L.; Velilla, I.; Ruzziconi, R.; Schindler, B. D.; Seo, S. M.; Kaatz, G. W.; Cruciani, G. *J. Med. Chem.* **2016**, *59*, 867–891; (c) Stec, J.; Onajole, O. K.; Lun, S.; Guo, H.; Merenbloom, B.; Vistoli, G.; Bishai, W. R.; Kozikowski, A. P. *J. Med. Chem.* **2016**, *59*, 6232–6247; (d) Labrière, C.; Gong, H.; Finlay, B. B.; Reiner, N. E.; Young, R. N. *Eur. J. Med. Chem.* **2017**, *125*, 1–13.
20. (a) Dousson, C.; Alexandre, F.-R.; Amador, A.; Bonaric, S.; Bot, S.; Caillet, C.; Convard, T.; da Costa, D.; Lioure, M.-P.; Roland, A.; Rosinovsky, E.; Maldonado, S.; Parsy, C.; Trochet, C.; Storer, R.; Stewart, A.; Wang, J.; Mayes, B. A.; Musiu, C.; Poddesu, B.; Vargiu, L.; Liuzzi, M.; Moussa, A.; Jakubik, J.; Hubbard, L.; Seifer, M.; Standring, D. *J. Med. Chem.* **2016**, *59*, 1891–1898; (b) Li, X.; Gao, P.; Huang, B.; Zhou, Z.; Yu, Z.; Yuan, Z.; Liu, H.; Pannecouque, C.; Daelemans, D.; De Clercq, E.; Zhan, P.; Liu, X. *Eur. J. Med. Chem.* **2017**, *126*, 190–201.
21. (a) Han, Z.; Liang, X.; Wang, Y.; Qing, J.; Cao, L.; Shang, L.; Yin, Z. *Eur. J. Med. Chem.* **2016**, *116*, 147–155; (b) Yu, W.; Tong, L.; Hu, B.; Zhong, B.; Hao, J.; Ji, T.; Zan, S.; Coburn, C. A.; Selyutin, O.; Chen, L.; Rokosz, L.; Agrawal, S.; Liu, R.; Curry, S.; McMonagle, P.; Ingravallo, P.; Asante-Appiah, E.; Chen, S.; Kozlowski, J. A. *J. Med. Chem.* **2016**, *59*, 10228–10243.
22. Scuotto, M.; Abdelnabi, R.; Collarile, S.; Schiraldi, C.; Delang, L.; Massa, A.; Ferla, S.; Brancale, A.; Leyssen, P.; Neyts, J.; Filosa, R. *Bioorg. Med. Chem.* **2017**, *25*, 327–337.
23. Musella, S.; di Sarno, V.; Ciaglia, T.; Sala, M.; Spensiero, A.; Scala, M. C.; Ostacolo, C.; Andrei, G.; Balzarini, J.; Snoeck, R.; Novellino, E.; Campiglia, P.; Bertamino, A.; Gomez-Monterrey, I. M. *Eur. J. Med. Chem.* **2016**, *124*, 773–781.
24. Cihan-Üstündağ, G.; Gürsoy, E.; Naesens, L.; Ulusoy-Güzeldemirci, N.; Çapan, G. *Bioorg. Med. Chem.* **2016**, *24*, 240–246.
25. (a) Cameron, K. O.; Kung, D. W.; Kalgutkar, A. S.; Kurumbail, R. G.; Miller, R.; Salatto, C. T.; Ward, J.; Withka, J. M.; Bhattacharya, S. K.; Boehm, M.; Borzilleri, K. A.; Brown, J. A.; Calabrese, M.; Caspers, N. L.; Cokorinos, E.; Conn, E. L.; Dowling, M. S.; Edmonds, D. J.; Eng, H.; Fernando, D. P.; Frisbie, R.; Hepworth, D.; Landro, J.; Mao, Y.; Rajamohan, F.; Reyes, A. R.; Rose, C. R.; Ryder, T.; Shavnya, A.; Smith, A. C.; Tu, M.; Wolford, A. C.; Xiao, J. *J. Med. Chem.* **2016**, *59*, 8068–8081; (b) Chu, K.-F.; Yao, C.-H.; Song, J.-S.; Chen, C.-T.; Yeh, T.-K.; Hsieh, T.-C.; Huang, C.-Y.; Wang, M.-H.; Wu, S.-H.; Chang, W.-E.; Chao, Y.-S.; Lee, J.-C. *Bioorg. Med. Chem.* **2016**, *24*, 2242–2250.
26. (a) Félix, M. B.; de Souza, E. R.; de Lima, M. D. C. A.; Frade, D. K. G.; Serafim, V. D. L.; Rodrigues, K. A. D. F.; Néris, P. L. D. N.; Ribeiro, F. F.; Scotti, L.; Scotti, M. T.; de

Aquino, T. M.; Mendonça Junior, F. J. B.; de Oliveira, M. R. *Bioorg. Med. Chem.* **2016**, *24*, 3972–3977; (b) Pandey, S.; Chauhan, S. S.; Shivahare, R.; Sharma, A.; Jaiswal, S.; Gupta, S.; Lal, J.; Chauhan, P. M. S. *Eur. J. Med. Chem.* **2016**, *110*, 237–245.
27. Orban, O. C. F.; Korn, R. S.; Benítez, D.; Medeiros, A.; Preu, L.; Loaëc, N.; Meijer, L.; Koch, O.; Comini, M. A.; Kunick, C. *Bioorg. Med. Chem.* **2016**, *24*, 3790–3800.
28. (a) Lamie, P. F.; Ali, W. A. M.; Bazgier, V.; Rárová, L. *Eur. J. Med. Chem.* **2016**, *123*, 803–813; (b) Liu, Z.; Tang, L.; Zhu, H.; Xu, T.; Qiu, C.; Zheng, S.; Gu, Y.; Feng, J.; Zhang, Y.; Liang, G. *J. Med. Chem.* **2016**, *59*, 4637–4650; (c) Pedada, S. R.; Yarla, N. S.; Tambade, P. J.; Dhananjaya, B. L.; Bishayee, A.; Arunasree, K. M.; Philip, G. H.; Dharmapuri, G.; Aliev, G.; Putta, S.; Rangaiah, G. *Eur. J. Med. Chem.* **2016**, *112*, 289–297; (d) Arnsmann, M.; Hanekamp, W.; Elfringhoff, A. S.; Lehr, M. *Eur. J. Med. Chem.* **2017**, *125*, 1107–1114; (e) Levoin, N.; Labeeuw, O.; Billot, X.; Calmels, T.; Danvy, D.; Krief, S.; Berrebi-Bertrand, I.; Lecomte, J.-M.; Schwartz, J.-C.; Capet, M. *Eur. J. Med. Chem.* **2017**, *125*, 565–572.
29. Zhu, W.; Bao, X.; Ren, H.; Da, Y.; Wu, D.; Li, F.; Yan, Y.; Wang, L.; Chen, Z. *Eur. J. Med. Chem.* **2016**, *115*, 161–178.
30. Temple, K. J.; Duvernay, M. T.; Young, S. E.; Wen, W.; Wu, W.; Maeng, J. G.; Blobaum, A. L.; Stauffer, S. R.; Hamm, H. E.; Lindsley, C. W. *J. Med. Chem.* **2016**, *59*, 7690–7695.
31. Sączewski, J.; Hudson, A.; Scheinin, M.; Wasilewska, A.; Sączewski, F.; Rybczyńska, A.; Ferdousi, M.; Laurila, J. M.; Boblewski, K.; Lehmann, A.; Watts, H.; Ma, D. *Eur. J. Med. Chem.* **2016**, *115*, 406–415.
32. (a) Benchekroun, M.; Romero, A.; Egea, J.; León, R.; Michalska, P.; Buendía, I.; Jimeno, M. L.; Jun, D.; Janockova, J.; Sepsova, V.; Soukup, O.; Bautista-Aguilera, O. M.; Refouvelet, B.; Ouari, O.; Marco-Contelles, J.; Ismaili, L. *J. Med. Chem.* **2016**, *59*, 9967–9973; (b) de Candia, M.; Zaetta, G.; Denora, N.; Tricarico, D.; Majellaro, M.; Cellamare, S.; Altomare, C. D. *Eur. J. Med. Chem.* **2017**, *125*, 288–298; (c) Lajarín-Cuesta, R.; Nanclares, C.; Arranz-Tagarro, J.-A.; González-Lafuente, L.; Arribas, R. *J. Med. Chem.* **2016**, *59*, 6265–6280; (d) Tarazi, H.; Odeh, R. A.; Al-Qawasmeh, R.; Yousef, I. A.; Voelter, W.; Al-Tel, T. H. *Eur. J. Med. Chem.* **2017**, *125*, 1213–1224.
33. Meredith, E. L.; Mainolfi, N.; Poor, S.; Qiu, Y.; Miranda, K.; Powers, J.; Liu, D.; Ma, F.; Solovay, C.; Rao, C.; Johnson, L.; Ji, N.; Artman, G.; Hardegger, L.; Hanks, S.; Shen, S.; Woolfenden, A.; Fassbender, E.; Sivak, J. M.; Zhang, Y.; Long, D.; Cepeda, R.; Liu, F.; Hosagrahara, V. P.; Lee, W.; Tarsa, P.; Anderson, K.; Elliott, J.; Jaffee, B. *J. Med. Chem.* **2015**, *58*, 9273–9286.
34. Guo, D.; Li, J.; Lin, H.; Zhou, Y.; Chen, Y.; Zhao, F.; Sun, H.; Zhang, D.; Li, H.; Shoichet, B. K.; Shan, L.; Zhang, W.; Xie, X.; Jiang, H.; Liu, H. *J. Med. Chem.* **2016**, *59*, 9489–9502.
35. Bertamino, A.; Ostacolo, C.; Ambrosino, P.; Musella, S.; Di Sarno, V.; Ciaglia, T.; Soldovieri, M. V.; Iraci, N.; Fernandez Carvajal, A.; de la Torre-Martinez, R.; Ferrer-Montiel, A.; Gonzalez Muniz, R.; Novellino, E.; Taglialatela, M.; Campiglia, P.; Gomez-Monterrey, I. *J. Med. Chem.* **2016**, *59*, 2179–2191.
36. Genin, M. J.; Bueno, A. B.; Agejas Francisco, J.; Manninen, P. R.; Bocchinfuso, W. P.; Montrose-Rafizadeh, C.; Cannady, E. A.; Jones, T. M.; Stille, J. R.; Raddad, E.; Reidy, C.; Cox, A.; Michael, M. D.; Michael, L. *J. Med. Chem.* **2015**, *58*, 9768–9772.
37. Saavedra, O. M.; Karila, D.; Brossard, D.; Rojas, A.; Dupuis, D.; Gohier, A.; Mannoury la Cour, C.; Millan, M. J.; Ortuno, J.-C.; Hanessian, S. *Bioorg. Med. Chem.* **2017**, *25*, 38–52.
38. Gurer-Orhan, H.; Karaaslan, C.; Ozcan, S.; Firuzi, O.; Tavakkoli, M.; Saso, L.; Suzen, S. *Bioorg. Med. Chem.* **2016**, *24*, 1658–1664.
39. Rao, Y.; Liu, H.; Gao, L.; Yu, H.; Ou, T.-M.; Tan, J.-H.; Huang, S.-L.; Wang, H.-G.; Li, D.; Gu, L.-Q.; Ye, J.-M.; Huang, Z.-S. *J. Med. Chem.* **2015**, *58*, 9395–9413.
40. Kumar, V.; Bonifazi, A.; Ellenberger, M. P.; Keck, T. M.; Pommier, E.; Rais, R.; Slusher, B. S.; Gardner, E.; You, Z.-B.; Xi, Z.-X.; Newman, A. H. *J. Med. Chem.* **2016**, *59*, 7634–7650.
41. (a) Gotor-Fernández, V.; Fernández-Torres, P. *Tetrahedron: Asymmetry* **2006**, *17*, 2558–2564; (b) Alatorre-Santamaria, S.; Rodriguez-Mata, M.; Gotor-Fernandez, V.; de Mattos, M. C.; Sayago, F. J.; Jimenez, A. I.; Cativiela, C.; Gotor, V. *Tetrahedron: Asymmetry* **2009**, *19*, 1714–1719; (c) Lopez-Iglesias, M.; Busto, E.; Gotor, V.; Gotor-Fernandez, V. *J. Org. Chem.* **2012**, *77*, 8049–8055.
42. López-Iglesias, M.; Arizpe, A.; Sayago, F. J.; Gotor, V.; Cativiela, C.; Gotor-Fernández, V. *Tetrahedron* **2016**, *72*, 7311–7316.
43. Busto, E.; Martínez-Montero, L.; Gotor, V.; Gotor-Fernández, V. *Eur. J. Org. Chem.* **2013**, *2013*, 4057–4064.
44. (a) Koskinen, A. M. P.; Klibanov, A.M. (Eds.) *Enzymatic Reactions in Organic Media*, 1rd ed. Springer Science+Business Media Dordrecht, 1996.; (b) Klibanov, A. M. *Nature* **2001**, *409*, 241–246.
45. Chen, C. S.; Fujimoto, Y.; Girdaukas, G.; Sih, C. J. *J. Am. Chem. Soc.* **1982**, *104*, 7294–7299.
46. Donohue, T. M.; Tuma, D. J.; Sorrell, M. F. *Arch. Biochem. Biophys.* **1983**, *220*, 239–246.
47. (a) Seco, J. M.; Quiñoá, E.; Riguera, R. *Tetrahedron: Asymmetry* **2001**, *12*, 2915–2925; (b) Seco, J. M.; Quiñoá, E.; Riguera, R. *Chem. Rev.* **2004**, *104*, 17–117; (c) Louzao, I.; Seco, J. M.; Quiñoá, E.; Riguera, R. *Chem. Commun.* **2010**, *46*, 7903–7905; (d) Seco, J. M.; Quinoa, E.; Riguera, R. *Chem. Rev.* **2012**, *112*, 4603–4641; (e) Mishra, S. K.; Suryaprakash, N. *Tetrahedron: Asymmetry* **2017**, *28*, 250–256.
48. (a) Bian, G.; Fan, H.; Huang, H.; Yang, S.; Zong, H.; Song, L.; Yang, G. *Org. Lett.* **2015**, *17*, 1369–1372; (b) Puentes, C. M.; Wenzel, T. J. *Beilstein J. Org. Chem.* **2017**, *13*, 43–53.
49. (a) Bal, D.; Gradowska, W.; Gryff-Keller, A. *J. Pharm. Biomed. Anal.* **2002**, *28*, 1061–1071; (b) Ghosh, I.; Zeng, H. B.; Kishi, Y. *Org. Lett.* **2004**, *6*, 4715–4718; (c) Adams, C. M.; Ghosh, I.; Kishi, Y. *Org. Lett.* **2004**, *6*, 4723–4726.
50. Wenzel, T. J.; Chisholm, C. D. *Chirality* **2011**, *23*, 190–214.
51. (a) Freedman, T. B.; Cao, X.; Dukor, R. K.; Nafie, L. A. *Chirality* **2003**, *15*, 743–758; (b) Burgueño-Tapia, E.; Chávez-Castellanos, K.; Cedillo-Portugal, E.; Joseph-Nathan, P. Tetrahedron: Asymmetry 2017, 28, 166–174.
52. (a) Li, X.; Tanasova, M.; Vasileiou, C.; Borhan, B. *J. Am. Chem. Soc.* **2008**, *130*, 1885–1893; (b) Li, X.; Borhan, B. *J. Am. Chem. Soc.* **2008**, *130*, 16126–16127; (c) Li, X.; Burrell, C. E.; Staples, R. J.; Borhan, B. *J. Am. Chem. Soc.* **2012**, *134*, 9026–9029.
53. He, Y.; Wang, B.; Dukor, R. K.; Nafie, L. A. *Appl. Spectrosc.* **2011**, *65*, 699–723.
54. Wagner, A. J.; Rychnovsky, S. D. *J. Org. Chem.* **2013**, *78*, 4594–4598.
55. Hoye, T. R.; Jeffrey, C. S.; Shao, F. *Nat. Protoc.* **2007**, *2*, 2451–2458.
56. Borowiecki, P.; Milner-Krawczyk, M.; Plenkiewicz, J. *Beilstein J. Org. Chem.* **2013**, *9*, 516–525.
57. (a) Borowiecki, P.; Poterała, M.; Maurin, J.; Wielechowska, M.; Plenkiewicz, J. *ARKIVOK* **2012**, *viii*, 262–281; (b) Borowiecki, P.; Milner-Krawczyk, M.; Brzezińska, D.; Wielechowska, M.; Plenkiewicz, J. *Eur. J. Org. Chem.* **2013**, *2013*, 712–720.
58. Borowiecki, P.; Fabisiak, M.; Ochal, Z. *Tetrahedron* **2013**, *69*, 4597–4602.
59. Borowiecki, P.; Paprocki, D.; Dranka, M. *Beilstein J. Org. Chem.* **2014**, *10*, 3038–3055.
60. Latypov, S. K.; Seco, J. M.; Quiñoá, E.; Riguera, R. *J. Org. Chem.* **1995**, *60*, 504–515.
61. Tschúgaeff, L. *Ber. Dtsch. Chem. Ges.* **1898**, *31*, 1775–1782.
62. Kazlauskas, R. J.; Weissfloch, A. N. E.; Rappaport, A. T.; Cuccia, L. A. *J. Org. Chem.* **1991**, *56*, 2656–2665.
63. Bradley, D.; Williams, G.; Lawton, M. *J. Org. Chem.* **2010**, *75*, 8351–8354.
64. Agilent Technologies, CrysAlisPro, Version 1.171.35.21b.
65. Sheldrick, G. M. *Acta Crystallogr.* **2008**, *64A*, 112–122.